LUND UNIVERSITY

Operational stability of lean premixed combustion in gas turbines

an experimental study on gaseous alternative fuels

Sayad, Parisa

2016

[Link to publication](#)

Operational Stability of
Lean Premixed Combustion in
Gas Turbines
An Experimental Study on Gaseous Alternative Fuels

DOCTORAL DISSERTATION

Parisa Sayad

Division of Thermal Power Engineering, Department of Energy Sciences
Faculty of Engineering, LTH, Lund University

Lund, Sweden, 2016

LUND
UNIVERSITY

i

Cover photo: OH*-chemiluminescence of top view of flame flashback in the variable-swirl burner

To the memory of my father,
for all the roads he guided me through…

To my son,
for all the days to look forward to…

iv

Popular Science Description

World electricity consumption is drastically increasing. One of the most common ways of producing electricity is to use the chemical energy of fossil fuels. This can be done in thermal power plants in which the chemical energy of fossil fuels such as natural gas is converted to mechanical energy and finally to electricity. Extracting the chemical energy of fuels is done through combustion of the fuel with air. Combustion produces heat, water and carbon dioxide as its main products. The produced heat can be converted to mechanical energy in different ways. In gas turbines, the hot combustion products are directly used to move turbine blades and produce mechanical energy, which is then converted to electricity by means of an electric generator. However, one should bear in mind that electricity is not the only outcome of this process. During this process, we are consuming the very limited reserves of fossil fuels, we are producing pollutants and we are negatively contributing in the climate change by producing carbon dioxide.

These negative consequences are becoming increasingly alarming. These concerns have led to a growing interest in the use of alternative fuels such as bio- and electro-fuels with reduced environmental impact for electricity production. Using bio- and electro-fuels in gas turbines provide reliable production of heat and electricity while decreasing the dependency on fossil fuels and contributing to the reduction of greenhouse gas emissions.

One of the most promising gaseous bio-fuels for gas turbines is digestion gas or 'biogas. Biogas contains varying amounts of CH_4 and CO_2 as its major components. Another alternative fuel that can be considered for gas turbine combustors is synthesis gas (syngas) fuels that can be produced from renewable sources such as lignocellulosic biomass. Syngas may contain H_2, CO, and CH_4, as well as CO_2, N_2, H_2O, and small amounts of higher hydrocarbons. The composition of these alternative fuels differs from natural gas, which has CH_4 as its main component. This means that these fuels have different chemical and physical properties and therefore different combustion properties than natural gas. Therefore utilizing such fuels as the main or part of the fuel mixture in gas turbine combustors may substantially affect their efficiency, operability and emission characteristics. It is thus important to understand and quantify their operational characteristics to make their use in gas turbines viable.

One of the most important aspects of combustion that has to be considered in gas turbines when using alternative fuels is operational stability. It means that the

combustion needs to take place in the combustor and in a smooth, reliable manner. In other words, the combustion needs to be sustained under all operating conditions. This is particularly important in modern gas turbines, referred to as lean premixed combustors, where fuel and air are mixed before entering the combustor. There are several operability risks that can occur and should be avoided in a lean premixed gas turbine combustor such as: lean blowout (the flame can extinguish due to reactions taking place too slowly), flashback (the flame can travel in to the premixing section), and autoignition (the fuel/air mixture can autoignite in the premixing section and before entering the combustor).

In this work, an experimental approach was used to investigate and understand the combustion of various fuel mixtures that can replace natural gas in gas turbines. A model combustor was designed and built that can mimic a real gas turbine combustor. The focus of the experiments was to investigate the combustion stability in the combustor when burning fuels comprising H_2, CO and CO_2. The combustor featured a quartz glass tube that provided optical access to the flame. Different experimental techniques were used to shed light on how the combustion behavior and operational stability of such fuels differs from natural gas. Various operating conditions and burner characteristics were examined in order to explore the possibility of reaching a fuel-flexible combustor.

Abstract

This doctoral thesis presents experimental investigations of operability risks of lean blowout, flashback and autoignition posed by using alternative fuels in premixed gas turbine combustors. The work focused on three main subjects: First, the lean blowout and flashback limits of various fuel mixtures in an atmospheric variable-swirl combustor were measured. Second, the influence which the combustor flow field had on the lean blowout and flashback limits was measured and analyzed. Third, the autoignition delays of various fuel/air mixtures were measured at different temperatures and pressures under turbulent flow conditions.

The lean blowout and flashback investigations aimed at identifying the effects of fuel composition on the lean blowout and flashback limits of the combustor under various operational conditions. The fuel mixtures studied, consisted of H_2, CH_4, CO, CO_2 and N_2 in varying proportions. The operational conditions were altered by varying swirl number, air inlet temperature and mass flow rate. Swirl number was varied between 0.00 and 0.66 by changing the proportion of tangential flow to axial flow through a swirl mixer located upstream of the combustor. The velocity profiles obtained from LDA measurements indicated that varying the swirl number from 0.00 to 0.66, drastically changed the flow field in the combustor. At swirl numbers greater than 0.53, a central recirculation zone was present in the combustor

Lean blowout experiments showed that swirl number played a major role in the flame structure and stabilization mechanism. In addition, the flame response to decreasing equivalence ratio was greatly influenced by the swirl number. Nonetheless, swirl number did not affect the lean blowout limit significantly specially for fuel mixtures with higher reactivity e.g. due to a higher H_2 content.

Flashback experiments showed that swirl number had a strong influence not only on the flashback limit but also on the mechanism that triggered flashback for a given fuel mixture. In the studied ranges of air mass flow rate and swirl number, four flashback mechanisms were identified: flashback due to combustion induced vortex breakdown (CIVB), flashback in the boundary layer, flashback due to autoignition and flashback in the core flow. In the case of flashback caused by autoignition, the ignition delay obtained from chemical kinetics calculations was an order of magnitude longer than the average residence time in the current experimental setup. Autoignition experiments in the flow reactor performed along with chemical kinetic calculations, suggested that catalytic effects of the reactor

walls might contribute in shortening the ignition delays, which poses the risk of autoignition under normal operation.

Comparing lean blowout and flashback limits of several fuel mixtures at swirl numbers of 0.53 and 0.66 indicated that even a minor change in the swirl number in the moderate range can result in significant enhancement of the operational stability range of the combustor when using highly reactive fuels. Further PIV velocity measurements using particle image velocimetry, suggested that the flashback mechanism was altered when reducing the swirl number from 0.66 to 0.53, which may be the underlying reason for the significant difference in flashback limits at theses swirl numbers.

viii

Acknowledgements

I would like to express my appreciation towards my supervisor, Professor Jens Klingmann for giving me the opportunity to work as a PhD student in his group and for providing me with professional guidance during my studies. Thank you for always being open to listen to and discuss my ideas, questions, confusions, concerns and even disappointments along the way. I have learned so much from you. Thank you for making me feel fully supported and independent at the same time.

I would like to thank Dr. Alessandro Schönborn not only for being my co-supervisor but also for being a tremendous mentor, a patient teacher, a fun colleague and a true friend. I am truly grateful for having your full support in every single step I took during my PhD studies. Thank you for guiding me through the wonderland of experimental research. You taught me to be more determined in making things work in lab than a hydrogen flame that is about to flashback. Your enthusiasm and love for research was indeed contagious. You finally made me fit into the definition of an experimental geek who becomes excited about a little blue flame jumping up and down. I must admit I even enjoy window shopping in BILTEMA and looking at screwdrivers and Swagelok fittings.

I would like to thank my co-supervisor Marcus Thern for the fruitful thermodynamic discussions. Thank you for always making time to answer my questions. I am truly grateful to you for always supporting me especially through the difficult times.

I would like to thank Professor Magnus Genrup for always being extremely generous in giving me confidence and positive feedback. I will never forget the brilliant experience I had as your teaching assistant. Your enthusiasm and interest in work in gas turbine research have given me a lot of motivation.

I would like to thank Catarina Linden for supporting me when I needed it most. I would like to thank our laboratory technicians: Ingjald, Kjel, Martin and Mats whose help has been crucial for performing my experiments.

I would like to thank my fellow PhD students, Ivan, Majed, Atanu and Srikanth for the fun discussions and the after work drinks. Special thanks goes to Mao and Tong for helping me in lab during the long days (and nights) of running loud scary combustion experiments.

During my time in Lund, I have made amazing friends from all around the world with whom I shared many memorable days. Björn, you are an amazing person and a great friend who has aspired me in many ways. We have many good memories and I am sure there are more to look forward to. I will never forget that you actually danced in my 30th birthday party. Kostas, thanks for always looking out for me and for being so kind and supportive. I would have not survived without our countless hangouts. Emanuela, we had an amazing 6 months together and the day you left, I knew that I have made a friend for life no matter how far she is. Henning, thanks for our work discussions, our dynamic loud parties and especially for our Swedish midsummer together. Aurelia, thank you for always being there for me. Mohammad and Susann, thank you for your support and kindness and for our many fun lunches, dinners, drinks and coffees together. Maria, thank you for always being up for discussing important matters. Kat, you are an incredible friend. Our friendship was the most spontaneous, yet long-lasting friendships of all times. I can never thank you enough for what you have done for me. Your support and kindness have brightened my days when I needed it the most.

I would like to thank my beloved family and friends in Iran who have given me sincere love and support all these years.

Babayee, I am going to miss you every day for the rest of my life. You were the strongest person I have ever known. You taught me, no matter how hard life may become, I can always find something beautiful that is worth living for. And that was what helped me to survive your loss when I was miles away from home. No one else could ever make me feel as strong as you did. Your extraordinary desire for learning, reading and trying new ideas are the most precious qualities that I learned from you.

Maman, I love you so much. Thank you for bringing me to this world, for raising me in an infinity of love and care and for letting me peruse my dreams no matter how far they took me away from you. You always wanted and did the best for me. You taught me to aim high, try hard and never give up hope.

 Dadash Babak, you are the best brother anyone could wish for, but to me you are much more than that. You have always been my best role model for everything. No matter how difficult things may get, I feel reassured when I look up at you. I know I will always have Dadash Babak to rely on when times are rough.

Sepideh joon, you are more than a sister to me. You have helped me in so many ways for so long that I cannot imagine how my life would have been without you. Thank you for everything.

My lovely niece, Nazanin thank you for being such an amazing friend. You make me feel confident and young in a very special way. Nima, I am very proud of you and I cannot wait for you to read and criticize my thesis in a couple of years.

Farzaneh, my little sister, you are a gift to my life. Thank you for your sincere love and kindness.

x

Somayeh, my dearest friend, words cannot even begin to express how much I miss you and how many times I wished, you were here. You understand me more than anyone else does. Thanks for your deep unconditional friendship.

Hesam, my beloved husband, there are no words to convey how much I love you. Without you by my side, I would have not even started my PhD studies let alone making it to the finish line. You have helped me with my experiments, you have discussed my results with me, you have reviewed my papers, and you have offered me advice for my thesis. But all of these are only a small part of what I am grateful for. Thank you for always seeing the best in me, for reminding me to trust myself, for helping me to see the light during my darkest moments, for encouraging me to move forward, for magically calming me down when I was frustrated, for giving me hope when nothing seemed to work. You have been and will remain my professional mentor, my favorite colleague and my best friend.

Last but by no means the least, my little star, my son, Adrian. Feeling you move under my skin during the hard days of writing my last article was the only thing that kept me going and back then I had no idea how much joy was awaiting me in the future. Thanks for coming to my world and making me realize what life is really about.

List of Publications

Paper I

Parisa Sayad, Alessandro Schönborn, Denny Clerini, Jens Klingmann, ''Experimental investigation of methane lean blowout limit; effects of dilution, mass flow rate and inlet temperature'', ASME 2012 Gas Turbine India Conference, Mumbai, Maharashtra, India, Paper No. GTIndia2012-9742.

Paper II

Parisa Sayad, Alessandro Schönborn, Jens Klingmann, ''Experimental investigations of the lean blowout limit of different syngas mixtures in an atmospheric, premixed variable-swirl burner'', Energy & Fuels, 27 (5), pp 2783–2793, 2013.

Paper III

Parisa Sayad, Alessandro Schönborn, Mao Li, Jens Klingmann, ''Visualisation of different flashback mechanisms for H_2/CH_4 mixtures in a variable-swirl burner'', Journal of Engineering for Gas Turbines and Power, 137(3), pp. 301507/1-9, 2015.

Paper IV

Parisa Sayad, Alessandro Schönborn, Jens Klingmann, ''Experimental investigation of the stability limits of premixed syngas-air flames at two moderate swirl numbers'', Combustion and Flame, 164, pp. 270-282, 2016.

Paper V

Alessandro Schönborn, **Parisa Sayad**, Jens Klingmann, ''Influence of precessing vortex core on flame flashback in swirling hydrogen flames'', International Journal of Hydrogen Energy, 39, pp. 20233-20241, 2014.

Paper VI

Alessandro Schönborn, **Parisa Sayad**, Alexander A. Konnov, Jens Klingmann, ''Visualisation of propane autoignition in a turbulent flow reactor using OH*-

chemiluminescence imaging'', Combustion and Flame, 160(6), pp. 1033-1043, 2013.

Paper VII

Alessandro Schönborn, **Parisa Sayad**, Alexander A. Konnov, Jens Klingmann, ''OH*-chemiluminescence during autoignition of hydrogen with air in a pressurised turbulent flow reactor'', International Journal of Hydrogen Energy, 39(23), pp. 12166-12181, 2014.

Related publications

Paper VIII

Alessandro Schönborn, **Parisa Sayad**, Alexander A. Konnov, Jens Klingmann, ''Autoignition of dimethyl ether and air in an optical flow-reactor'', Energy & Fuels, 28(6), pp. 4130-4138, 2014.

Paper IX

Ward De Paepe, **Parisa Sayad**, Svend Bram, Jens Klingmann, Francesco Contino, ''Experimental investigation of the effect of steam dilution on the combustion of methane for humidified micro gas turbine applications'', Combustion Science and Technology'', 188(8), pp. 1199-1219, 2016.

Contents

Nomenclature

A	Cross section area	m^2
A_I	Interrogation area	$pixel^2$
C_{quench}^*	Critical quench constant	-
D	Diameter of the premixing section	m
$D_{e^{-2}}$	Diameter of the laser beam in Eq. 20-21	m
Da	Damköhler number	-
d_f	Fringe spacing	m
d_m	Diameter of the measurement volume	m
dt	Change in time	s
dx	Change in axial distance	m
E	Activation energy	$kJ/mole$
f	Focal length of the focusing lens	m
f_c	Centrifugal force	$kg.m/s^2$
G_a	Axial flux of axial momentum	$kg.m/s^2$
G_t	Axial flux of tangential momentum	$kg.m^2/s^2$
$I_1(x), I_2(x)$	Light intensities in the interrogation area of the first and second frames in PIV	$J/m^2/s$
Ka	Karlovitz number	-
l_0	Integral length scale	m
l_m	Length of the measurement volume	m
Le_F	Lewis number of the fuel mixture	-
$\dot{m}$	Mass flow rate	$SLPM$
p	Static pressure	bar
r	Radial coordinate	m
R	Radius of the swirler	m

R_u	Universal gas constant	$J/mole/K$
Re_{l_0}	Reynolds number based on integral length scale	-
S	Swirl number	-
S_L	Laminar flame speed	m/s
S_T	Turbulent flame speed	m/s
T	Temperature	K
$\vec{U}$	Velocity vector	m/s
U	Axial velocity	m/s
u'	Turbulent velocity fluctuation	m/s
U_b	Bulk velocity in the premixing section	m/s
U_f	Incoming flow velocity after autoignition	m/s
U_i	Incoming flow velocity prior to autoignition	m/s
V	Volume	m^3
W	Tangential (Azimuthal) velocity	m/s
Y	Mass fraction	-

Greek symbols

α	Thermal diffusivity	m^2/s
α	Half angle between two laser beams in Eq. (17) and (19-21)	rad
η	Kolmogorov length scale	m
δ_L	Laminar flame thickness	m
Δt	Time step	s
ΔV	Change in volume of the gasses	m^3
λ_0	Wave length of the light source in Eq. (17)	m
ρ	Density	kg/m^3
ρ_u	Unburned gas density	kg/m^3
ρ_b	Burned gas density	kg/m^3
τ	Ignition delay	ms

τ_{chem}	Chemical time scale	s
τ_{l_0}	Integral time scale	s
τ_{PSR}	Residence time of a PSR	s
τ_{res}	Residence time	s
$\tau_{transient}$	Residence time of a transient PSR	s
τ_η	Kolmogorov time scale	s
u_η	Kolmogorov velocity	m/s
υ	Kinematic viscosity	m^2/s
ϕ	Equivalence ratio	-
$\vec{\omega}$	Azimuthal vorticity	$1/s$
ω_1, ω_2	Frequency of two scattered light waves	Hz
ω_D	Doppler frequency	Hz

Abbreviations

BL	Boundary Layer
BSA	Burst Spectrum Analyzer
CCD	Charge Couple Device
CIVB	Combustion Induced Vortex Breakdown
FB	Flashback
IEA	International Energy Agency
IGCC	Integrated Gasification Combined Cycle
LBO	Lean Blowout
LDA	Laser Doppler Anemometry
PIV	Particle Image Velocimetry
PVC	Precessing Vortex Core

Chemical compounds

C_3H_8	Propane
CH_4	Methane
CO	Carbon monoxide
CO_2	Carbon dioxide
H_2	Hydrogen
H_2O	Water
HO_2	Hydrodioxide
N_2	Nitrogen

NO_X	Nitrogen oxides
O_2	Oxygen
OH^*	Hydroxide
TiO_2	Titanium dioxide

xx

1. INTRODUCTION

1.1. Motivations

The world electricity consumption is drastically increasing. According to the International Energy Agency (IEA), fossil fuel-powered plants produce the largest share of the world's electricity [1]. The ever-increasing dependency on fossil fuels has raised world-wide concerns about the continued availability of fossil fuel resources. In 2005, IEA found that the known fossil fuel resources existing around the globe are sufficient to meet the increasing energy demand for the foreseeable future [2]. However as the main source of greenhouse gases, combustion of fossil fuels have the largest contribution in climate change [3]. Thereby the primary constrain on having continued access to fossil fuels is thought to be their long-term environmental damage. This has led to a growing interest in the use of alternative fuels such as bio- and electro-fuels with reduced environmental impact for energy production.

Renewable sources such as wind and solar energy are expected to have an increasing contribution in energy production. However, gas turbines, as reliable energy production units, will continue to have a significant role in the future [4]. Using bio- and electro-fuels in gas turbines can provide reliable production of heat and electricity while decreasing the dependency on fossil fuels and contributing to the reduction of greenhouse gas emissions.

Bio-fuels are referred to fuels that are obtained from biological material and can include bio-diesel, bio-alcohol, low-calorific-value gasified biomass, synthesis gas, etc. [5]. Using technologies such as Integrated Gasification Combined Cycles (IGCC) can enable combustion of biofuels in gas turbines.

Electro-fuels have been proposed as a solution to capture the electrical energy produced from intermittent renewable sources such as wind and solar power and store it in the form of chemical energy in liquid and gaseous fuels. Hydrogen is one of the electro-fuels that has the potential to be introduced into natural gas grids for power production [6].

Due to having different compositions, the chemical and physical properties of bio- and electro-fuels vary significantly from natural gas in terms of their heating values, ignition delays and transport properties. These differences can lead to notable differences in combustion behavior of these fuels compared with natural gas. Therefore, utilizing such fuels as the main or part of the fuel mixture in gas

1

turbine combustors can affect the efficiency, operability and emission characteristics of the unit substantially. It is thus important to understand and quantify their operational characteristics to make their use in gas turbines viable.

1.2. Background

Until the last few decades, diffusion-type combustors were employed in gas turbines [4]. In diffusion-type combustors, fuel and air are introduced into the combustor primary zone as separate streams. This approach produces a stable flame which is sustained in high-temperature zones where the fuel and air are mixed. Due to the absence of oxidizer in the fuel stream, the flame cannot propagate into the fuel supply lines. This makes diffusion-type combustors a relatively trouble-free choice for gas turbines which can accommodate moderate changes in fuel composition. However, diffusion-type combustors are poor candidates for low-emission power production due to their high NO_X emissions. NO_X is produced through the thermal pathway in the high-temperature reaction zone of diffusion flames.

Lean premixed combustion has been introduced in land-based gas turbine technology as a solution for emission reduction [7]. Mixing of fuel and air before combustion allows for operating the reaction zone at a lean fuel/air ratio. This reduces the combustion temperature and thus the formation of thermal NO_x through the thermal pathway. Lean, premixed combustors are however more prone to operability issues. Operating at lean fuel/air ratios creates the risk of flame blowout, particularly at part-load or start-up conditions due to low temperatures. On the other hand, since the fuel and air are premixed prior to entering the combustor, the fuel/air mixture can autoignite before reaching the combustor. In addition, since in lean premixed combustors the flame stabilization is primarily achieved by an aerodynamically induced recirculating flow [8], the flame can flashback from the combustor into the premixing section as a result of changes in the operating conditions. Flashback can severely disrupt the operation of the system and lead to disastrous structural damage.

These issues show that, operability risks related to flame stabilization have made lean premixed combustors sensitive to fuel choices. Current low-emission lean premixed combustors are mainly optimized for operation on natural gas. Therefore developing fuel-flexible combustors requires extensive investigations of the combustion behavior of unconventional fuels. Modern gas turbines fueled with such gases should have similar, reliable operation and low pollutant emissions as their natural-gas-fired counterparts.

1.3. Aim and Objectives

Combusting fuels with physical and chemical properties that are substantially different from natural gas in gas turbine combustors may significantly alter their performance, and cause operability problems such as lean blowout, flashback and autoignition. The aim of this study was to investigate the operability issues associated with using alternative fuels in premixed gas turbine combustors. To this end, the research objectives of this work were:

- To measure and compare the lean blowout and flashback limits of various fuel mixtures of biogas, syngas, diluted syngas, diluted methane and hydrogen-enriched methane.
    - To investigate how different components of the fuel mixtures affect the lean blowout and flashback limits.
    - To investigate the usefulness of the chemical kinetic models in predicting or correlating the experimentally obtained lean blowout and flashback limits of various fuel mixtures in a given experimental setup.
- To study the influence of the combustor flow field on combustion behavior of various fuel compositions particularly close to their lean blowout and flashback limits.
    - To study the influence of different flow field parameters such as temperature, mass flow rate and swirl number on the lean blowout and flashback limits as well as on the mechanisms driving them for a given fuel mixture.
    - To study the effect of varying the swirl number on the velocity field and flame stabilization mechanism in the combustor for a given fuel mixture.
    - To investigate whether certain flow field parameters such as swirl number can be used to improve lean blowout and flashback propensity of different fuels.
- To study the autoignition of various fuel/air mixtures in a turbulent flow reactor under conditions similar to a gas turbine premixer.
    - To visualize the initiation and propagation of autoignition for various fuels.
    - To measure the ignition delay of various fuels under varying conditions.
    - To calculate the ignition delays of the tested fuel/air mixtures using chemical kinetics models.
    - To compare the chemical kinetic calculations with the experimental results and explain the observed deviations.

Pursuing the above mentioned research objectives formed the framework for this doctoral thesis and led to seven published peer-reviewed articles.

1.4. Approach

To perform experimental investigation of lean blowout, flashback and autoignition in lean premixed combustion, two experimental setups were used throughout this work:

- ***An atmospheric variable-swirl combustor*** was used to study the lean blowout and flashback of different fuel mixtures. Using an optically accessible combustor enabled visual investigation of the flame at different conditions. The flow field in the combustor was varied by changing the swirl strength of the flow entering the combustor. Other inlet conditions that were varied during different experiments were air inlet temperature and inlet air mass flow rate.
- ***A pressurized turbulent continuous-flow reactor*** was used to study the autoignition of different fuel/air mixtures.

During the experimental investigations, the following measurement techniques were used to provide better understanding of the observations:

- Laser Doppler anemometry (LDA) was used to measure the velocity profiles at the inlet of the combustor in order to determine the swirl number in the variable-swirl combustor.
- CO emission measurements were performed during lean blowout experiments to determine the proximity of lean blowout limit.
- High-speed OH^*-chemiluminescence imaging was used in flashback experiments to visualize the flame propagation from the combustor into an optically accessible premixing section for various fuel mixtures at different flow conditions.
- High-speed particle image velocimetry (PIV) measurements were used to characterize the flow field in the combustor at different swirl numbers during stable operation as well as when flashback limit was approached.
- High-speed OH^*-chemiluminescence imaging was used to visualize the occurrence of autoignition in the optical test section of the flow reactor.

In addition to experimental investigations, chemical kinetic calculations were performed to understand the contribution of chemical kinetics in the results obtained from lean blowout, flashback and autoignition experiments.

4

1.5. Thesis outline

The thesis is organized as a collection of papers that have been produced during this project. The introductory overview of the topic is presented in the thesis in 7 chapters followed by the publications:

❖ **Chapter 1** gives an introduction to the thesis. Motivations, background, objectives of the thesis as well as the approaches used to perform the study are presented in this chapter.

❖ **Chapter 2** provides a theoretical background on swirl-stabilized gas turbine combustors. The stability issues related to lean premixed combustors are described in this chapter. Alternative fuels with relevance to gas turbine application are discussed with a brief literature review on previous studies.

❖ **Chapter 3** offers a brief introduction on the chemical kinetic modeling in premixed combustion followed by a summary of the chemical kinetic modeling work that was conducted throughout this thesis.

❖ **Chapter 4** presents the experimental setups used throughout the project.

❖ **Chapter 5** provides a description of the measurement techniques used in conducting the experimental investigations.

❖ **Chapter 6** presents the highlights of the results followed by a summary of the publications.

❖ **Chapter 7** provides the concluding remarks of the work followed by some suggestions for future research.

6

2. THEORY

2.1. Turbulent premixed combustion

Turbulent premixed flames are of great interest due to their application in industrial systems such as gas turbines or internal combustion engines. Operating lean premixed gas turbine combustors at high turbulence levels can help to achieve an efficient combustion in a compact geometry. Turbulence enhances mixing and turbulent flames have burning rates that are significantly higher than laminar flames. It is therefore possible to combust high amount of fuel/air mixtures efficiently in a small volume. However, turbulence brings a lot of complexity to the combustion process.

Turbulence consists of a range of time and length scales which can interact with the flame structure in different ways. The flow and turbulent structures are also strongly affected by the flame due to the large gradients of temperature, density and viscosity across the flame. Due to this strong coupling between turbulence and combustion, turbulent premixed flames exhibit substantially different behavior than laminar premixed flames. While laminar flames can be characterized by thermochemical properties of the fuel/oxidizer mixture, the behavior of turbulent premixed flames is dependent on turbulence and chemical time and length scales as well as on the thermochemical properties of the fuel/oxidizer mixture. Nevertheless, it is customary to use laminar flame characteristics to isolate the chemical and thermal processes occurring in turbulent premixed flames. Two important parameters that are used to characterize the laminar premixed flames are laminar flame speed (S_L) and laminar flame thickness (δ_L). S_L is defined as the time it takes for a laminar flame to propagate over a distance of one flame thickness. δ_L is defined as a distinct reaction zone in the flame where most of the reactions take place. The reaction zone of laminar premixed flames can be divided into a preheat zone, an inner reaction (fuel consumption) zone and an oxidization zone. The preheat zone is where the fuel and oxidizer are preheated prior to reaction. The temperature in preheat zone is raised mainly due to the diffusion of heat that is released in the inner reaction zone. The inner reaction zone is where the fuel and oxidizer react through many chain branching and chain propagating reactions. In the oxidization zone the remaining reactions between the intermediate species are completed [9].

2.1.1. Turbulent premixed flame regimes

One approach to describe the interaction between the flame and turbulence structures in turbulent premixed flames is to compare the chemical and turbulent time and length scales. To this end, three dimensionless numbers are often used to classify turbulent premixed flames into different regimes. The first two dimensionless numbers are Damköhler number (Da) and Karlovitz number (Ka) which both relate chemical and flow time scales. The Damköhler number is defined as the ratio between the integral time scale (τ_0) and the chemical time scale (τ_{chem}). The integral time scale can be expressed as the integral length scale (l_0), which is associated with the largest turbulent structures in the flow, divided by the turbulent velocity fluctuation (u'). The chemical time scale can be defined as the ratio between the laminar flame thickness (δ_L) and the laminar flame speed (S_L). The Damköhler number can therefore be written as:

$$Da = \frac{\tau_0}{\tau_{chem}} = \frac{l_0 S_L}{\delta_L u'} \tag{1}$$

The *Karlovitz* number relates the chemical time scale to the smallest turbulent time scale, *Kolmogorov* time scale (τ_η):

$$Ka = \frac{\tau_{chem}}{\tau_\eta} = \frac{\delta_L}{\eta} \frac{u_\eta}{S_L} = (\frac{l_0}{\delta_L})^{-\frac{1}{2}}(\frac{u'}{S_L})^{\frac{3}{2}} \tag{2}$$

The third dimensionless number is turbulent Reynolds number (Re_{l_0}) which relates the inertial forces to viscos forces and can be defined based on turbulent velocity fluctuation (u') and integral length scale (l_0):

$$Re_{l_0} = \frac{u' l_0}{v} \tag{3}$$

Depending on the values of the Reynolds, Damköhler and Karlovitz numbers, the behavior of turbulent premixed flames can be classified using the Borghi diagram shown in Figure 1. At turbulent Reynolds numbers below unity, the flame have laminar properties, which correspond to the bottom left corner of the Borghi diagram. The line $Da = 1$ denotes a boundary above which chemical time scale is larger than the turbulence time scale. This means that at $Da < 1$, chemical reactions are slower than turbulent mixing and the combustion is controlled by chemistry rather than by turbulence. This regime ($Da < 1$) is therefore called perfectly stirred reactor regime. $Ka = 1$ line is called Klimov-Williams criterion. Below this line where $Ka < 1$, the flame is in the flamelet regime where the flame is affected only by turbulent structures that are larger than the flame thickness. In other words, in this regime turbulence can only wrinkle the flame front without penetrating into the preheat zone or inner reaction zone. At $Ka < 1$, if $u' < S_L$, the regime is called wrinkled flamelets and if $u' > S_L$, the regime is called corrugated flamelets. As the Karlovitz number increases, turbulence has more influence on the flame structure.

8

In the regime characterized by $1 < Ka < 100$, the smallest turbulence structures can penetrate into the preheat zone but not the inner reaction zone of the premixed flames. This regime is called thin reaction zone. At $Ka > 100$, even the thin inner reaction zone of the flame will be influenced by the smallest turbulence structures. The regime in which the thin flame front can no longer be identified is called distributed reaction zone.

Real gas turbines operate at very high Reynolds numbers and high turbulence intensities. The smallest turbulence scales are very small and can interact with the inner reaction zone of the flame. Laboratory scaled combustors generally operate at lower Reynolds numbers with Karlovitz numbers around unity [9].
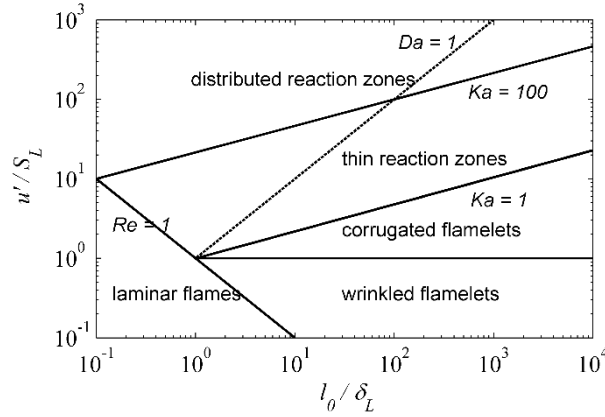

Figure 1.
Combustion diagram (Borghi diagram) for turbulent premixed combustion [10].

2.2. Swirl-stabilized combustors

Flame anchoring in lean premixed combustors is most often achieved aerodynamically by swirl-induced vortex breakdown. A swirl generator is placed upstream of the combustor which introduces an azimuthal (tangential) velocity to the flow. As presented in Eq. (4) [8], the azimuthal velocity generates a centrifugal force which produces a radial pressure gradient.

$$\frac{\partial p}{\partial r} = f_c = \rho \frac{W^2}{r} \tag{4}$$

where p is the static pressure, f_c is the centrifugal force, ρ is the density and W is the azimuthal velocity.

As the swirling flow passes through the sudden expansion at the entrance of the combustor, the radii of the stream-surfaces increase, which leads to a decrease

in the azimuthal velocity in stream-wise direction due to the conservation of angular momentum. The decrease in azimuthal velocity creates a positive pressure gradient along the axial axis. If the swirl strength of the flow is high enough, this leads to the formation of a recirculation zone in the combustor. The recirculation zone mixes a portion of the hot combustion products with incoming fresh reactants. This aerodynamic structure serves as a continuous source of ignition and acts as a flame stabilization mechanism. The flow in the recirculation zone is associated with high shear stresses and strong turbulence intensity, both of which are essential for flame stabilization and compactness of the flame.

2.2.1. Swirl number

Swirl in gas turbine combustors is commonly generated using axial or radial swirlers. These can be used as a single swirler or in a multiple arrangement to supply co-rotating or counter-rotating flows [11]. Depending on the amount of the rotational motion imparted to the flow, different flow patterns may emerge in the combustor. In order to characterize the relation between the strength of the swirl component and the axial component of the flow, a swirl number can be defined as in Eq. (5).

$$S = \frac{G_t}{R \, G_a} \tag{5}$$

where R is the radius of the swirler, G_t is the axial flux of the tangential momentum, and G_a is the axial flux of the axial momentum. These may be calculated as follows:

$$G_t = 2\pi \int_0^R \rho W U r^2 dr \tag{6}$$

$$G_a = 2\pi \int_0^R \rho U^2 r dr \tag{7}$$

where ρ is the density of the gas, U its axial velocity, W its tangential velocity and r is the radial coordinate [12].

It should be noted that even though swirl number has been considered as a significant criterion for swirling flows [12], swirling flows with the same swirl number may have different characteristics depending on the configuration of the swirler. For example, it was shown by Smith et al. [13] that despite having the same swirl number, radial swirlers produced a stronger recirculation zone in the combustor compared to their axial counterparts.

10

2.3. Stability issues

2.3.1. Lean blowout

Lean Blowout (LBO) describes the process of flame extinction under lean conditions, by means of the flame leaving its stable anchored position and being drawn downstream of the combustor where it extinguishes. In a gas turbine combustor, this is particularly likely to occur under part load conditions and during transient operation such as during turbine start-up. Blowout is usually avoided by the use of a pilot flame operated at richer conditions than the main flame, or as a diffusion flame, to provide a continuous source of ignition. The disadvantage of pilot flames is their higher combustion temperature, which is responsible for the increased formation of nitrogen oxides (NO_x). In practical applications, it is thus desirable to avert blowout through accurate knowledge of the blowout limits of the combustor instead of using pilot.

The current literature describes two theoretical approaches for the characterization of blowout [14-16]. The first approach is based on the assumption that blowout occurs under the condition where the residence time in the combustor is insufficient for the chemical reactions to take place. In this approach, a chemical time scale is compared with a flow time scale. The residence time is defined based on flow characteristics and the dimensions of the combustor. The chemical time scale can be estimated based on the laminar flame speed and thermal diffusivity of the mixture as presented in Eq. (8) [16, 17].

$$\tau_{chem} = \frac{\alpha}{S_L^2} \qquad (8)$$

Where α is the thermal diffusivity of the mixture. Another method to estimate the chemical kinetic time is to calculate the lean blowout residence time of a perfectly stirred reactor. The second approach considers the ratio of flame and flow speed. It is based on the assumption of flamelet-like combustion behavior, where blowout occurs when the flow speed exceeds the flame speed at critical locations within the combustor [18]. In either method, mixture diffusivity, heat content and kinetic characteristics of the fuels [19], as well as combustor flow field are critical for the prediction of blowout.

2.3.2. Flashback

Flashback occurs when the flame propagates upstream from the combustor into the premixing section. This can be a result of the turbulent flame speed exceeding the flow velocity along some streamlines in the combustor causing the reaction zone to

11

travel upstream. Several experimental investigations in the literature have shown that in swirling flows the mechanism driving flashback cannot be explained merely by the competition between the flame speed and flow velocities [20-24], but that flashback occurrence is strongly dependent on the flow field and the flame stabilization mechanism used in the combustor.

Four mechanisms with relevance to this work have been described in the literature. These may lead to flame propagation in the premixing section depending on the fuel composition, operating condition and the flow field in the combustor:

- *Flame propagation in the high-velocity core flow*
- *Flashback in the boundary layer (BL)*
- *Flashback due to combustion induced vortex breakdown (CIVB)*
- *Flame propagation in the premixing section caused by autoignition*

Flame propagation in the high-velocity core flow refers to the condition where the flame speed exceeds the flow velocity along some streamlines in the combustor causing the flame to propagate upstream into the premixing section. In highly turbulent swirling flows, the local axial flow velocities can be significantly lower than the mean velocity in the combustor, which may increase the risk of upstream flame propagation from the combustor into the premixing section. The occurrence of this type of flashback in gas turbine combustors is therefore dependent on the turbulent velocity fluctuations as well as fuel composition.

Flashback in the boundary layer refers to the condition where the flame propagates from the combustor into the premixing section through the low velocity regions close to the wall. Due to the no-slip boundary condition, the axial flow velocity increases from zero at the wall to the free stream velocity. This means that there may be a higher risk for the flame speed to exceed the flow velocity in the boundary layer and propagate upstream into the premixing section. However, similar to the axial flow velocity, the flame speed also decreases near the wall. This is because the chemical reactions cannot be sustained closer than a certain distance to the wall, because of the quenching due to the heat losses to wall. This distance is referred to as quenching distance. Flashback in the boundary layer will occur only if the flame speed exceeds the flow velocity at a certain distance within the boundary layer, which is greater than the quenching distance.

The boundary layer flashback was first introduced by Lewis and von Elbe [25] for laminar flames. They proposed that boundary layer flashback occurs when the velocity gradient of the flow falls below a critical velocity gradient. Wohl [26] further extended the critical gradient model emphasizing the effect of quenching. The boundary layer flashback in turbulent flames was studied by Yamazaki and Tsuji [27] who reported that the flashback limit could not be explained by the original concept of velocity gradient due to the very thin boundary layer in turbulent cases. In another study [28] the boundary layer flashback for both laminar and

12

turbulent flames was investigated reporting that at a constant pressure the critical boundary velocity gradient for turbulent flashback was significantly larger than that for laminar flashback. It was suggested that close to flashback conditions, a turbulent flame was stabilized in the laminar sub-layer, implying that a turbulent flame could penetrate about three times closer to the wall than a laminar flame. This was attributed to the fact that contrary to laminar flames, the heat transfer coefficient was not constant in the presence of turbulence and decreased from the turbulent core toward the wall.

Flashback due to combustion induced vortex breakdown (CIVB) occurs in swirling flames in which a recirculation zone with strong backflow of hot gases is used as flame stabilization mechanism. The axial position of the recirculation zone depends on the balance between the incoming positive axial velocity and the negative axial velocity in the recirculation zone. This balance can be disturbed due to the interaction between the flame and the recirculation zone, causing the stagnation point of the recirculation zone to move from the combustor into the premixing section. This creates a low velocity zone upstream of the flame, which consequently causes the flame to propagate into the premixing section. This mechanism for flashback in swirl-stabilized combustors has been referred to as Combustion Induced Vortex Breakdown (CIVB) and has been the subject of a number of studies [21, 29-33].

The interaction between the flame and the recirculation zone can be explained considering the azimuthal vorticity transport equation [34] which is presented in Eq. (9).

$$\frac{D\omega}{Dt} = \frac{\partial}{\partial t}(\vec{\omega}) + (\vec{U}.\nabla)\vec{\omega} = (\vec{\omega}.\nabla)\vec{U} - \vec{\omega}(\nabla.\vec{U}) + \frac{1}{\rho^2}(\nabla\rho \times \nabla p) \qquad (9)$$

In Eq. (9) $\vec{\omega}$ is the azimuthal vorticity, $\vec{U}$ is the velocity vector, ρ is the density and p is the static pressure.

Eq. (9) shows that azimuthal vorticity ω induces a velocity component against the main flow direction according to the law of Biot-Savart [35]. The heat release from the flame contributes to the production of azimuthal vorticity and can thereby affect the position of the recirculation zone in the combustor. The last two terms on the right-hand side of Eq. (9) correspond to the combustion-induced terms, namely volume expansion and baroclinic torque. The volume expansion leads to the production of positive azimuthal vorticity and thus to the reduction of the induced axial velocity against the incoming flow. The baroclinic torque on the contrary, produces negative azimuthal vorticity which leads to an induced axial velocity towards the incoming flow and can push the flame further upstream into the premixing section [32]. The density ratio across the flame is thus an important factor in governing the flame position and of its ability to flashback into the premixing section.

13

Flame propagation in the premixing section caused by autoignition occurs when the residence time of the fuel-air mixture in the premixing section exceeds the critical time necessary to cause autoignition. Plee and Mellor [36] argued that autoignition may occur in regions of flow separation of combustor premixing section, even under the conditions where the mean-flow residence time is shorter than the ignition delay of the fuel-air mixture. Beerer and McDonell [37] measured ignition delays of hydrogen under conditions comparable to those of gas turbine premixing sections. In their experiments they noted high temperatures along the walls of their reactor, even when autoignition had not taken place [37]. This pointed towards surface reactions taking place along the walls. The authors ascribed this to increased residence time of the reactants along the wall, and catalytic reactivity of the walls.

2.3.3. Autoignition

Autoignition may be defined as spontaneous ignition of a fuel/oxidizer mixture in the absence of any concentrated source of ignition such as a flame or spark [11]. Autoignition can happen in a premixed gas turbine combustor where the fuel and air are mixed prior to entering the combustor, if the residence time in the premixing section exceeds the ignition delay of the mixture. The sudden consumption of reactants in the premixing section can lead to blowout and flashback. These will in turn increase emissions, disturb turbine operation and may cause structural damage to the turbine.

Autoignition happens through a rapid spontaneous increase in the reaction rate of a combustible mixture that was initially in a slow reactive state. For small molecules such as hydrogen or methane, the majority of the reactions are usually highly exothermal and autoignition is accompanied by a strong rise in temperature. The reasons for the rapid increase in the reaction rates is twofold: First, the heat generated by exothermal reactions increases the reaction temperature and thereby accelerates the reaction rate. Second, the exponential multiplication of reactive species (radicals) through chain branching reactions accelerates the reaction rate. In practical combustion systems, autoignition of most fuels occurs as a result of both thermal and chain branching processes [38, 39]. The point of autoignition is usually defined by the maximum temperature increase over time or by the maximum concentration of reactive species such as the hydroxyl radical (OH^*). The time it takes for a given fuel/air mixture at a certain temperature and pressure to autoignite is referred to as ignition delay [40]. The ignition delay is a function of fuel/oxidizer composition, initial temperature and pressure.

Ignition delay of a given mixture can be correlated with pressure, temperature and the equivalence ratio of the mixture using an Arrhenius form for the reaction rate, assuming that the ignition delay is proportional to the inverse of the reaction rate [11]:

14

$$\tau = Ap^{-n}\phi^{-m}exp(\frac{E}{R_u T}) \tag{10}$$

where A, n and m are constants which are determined experimentally, p is the pressure, E is the activation energy, R_u is the universal gas constant and T is the initial temperature of the fuel/air mixture.

The ignition delay is a measure of reaction time and in its simplest form could be approximated by a single global reaction of fuel and oxidizer. In reality, the reaction between the fuel and oxidizer involves tens to hundreds of elementary overlapping reaction steps. These elementary reactions can be chain-initiating, chain-branching or chain-terminating occurring in gas phase or as surface reactions at the walls[39]. The elementary reactions can each be modelled as obeying the Arrhenius equation presented in Eq. (10). The ignition delays of different fuel/oxidizer mixtures can be determined using detailed chemical kinetic mechanisms that include the elementary reactions involved in the autoignition of a given fuel/air mixture [41].

In addition to the chemical reactions involved in autoignition, there are several physical processes such as mixing, turbulent interactions and heat loss to the walls that can influence the autoignition process and hence the ignition delay of a certain fuel/air mixture in a gas turbine combustor. In presence of flow in the system, such as in gas turbine combustors, the interaction between chemistry and fluid mechanics can influence the ignition delay of a given fuel/air mixture.

In order to predict the propensity for autoignition in a premixed gas turbine combustor, the ignition delay of the fuel/air mixture can be compared to the residence time of the fuel/air mixture in the premixing section before reaching the combustor. The mean residence time in the premixing section can be estimated by dividing the length of the premixer to the average velocity of the fuel/air mixture. Using a mean residence time does not account for flow complexities, which can exist in the premixer due to fuel injection, mixing process, swirling motion and flow separation.

Experimental autoignition studies may be carried out using a variety of techniques such as flow-reactors, rapid-compression machines and shock-tubes. Flow reactors provide the most accurate representation of the conditions encountered in gas turbine premixers, since they mimic their turbulent flow and near-constant pressure [42, 43]. Flow reactors typically consist of a long straight duct of circular cross section containing preheated reactants flowing through the duct. Fuel is injected near the beginning of the duct where it is rapidly mixed with air or a diluted oxidant by turbulent mixing and molecular diffusion. The fuel/oxidizer mixture chemically reacts as it flows downstream until it reaches the test section where the autoignition is expected to occur. To ensure that the mixture autoignites within the test section, mass flow rate and bulk velocities are adjusted depending on the composition, temperature and pressure of the mixture [44]. The chemical reactions are usually quenched after the test section using injection of

15

water or air. Flow reactors are typically able to operate at long autoignition times (100-500 ms) and low temperatures (600-1150 K) over a wide range of pressures (0.1-3 MPa) [45].

2.4. Alternative fuels for gas turbines

2.4.1. Hydrogen-containing fuels

Fuel mixtures comprising hydrogen are of increasing interest to power generation using gas turbines. Hydrogen can be produced remotely from solar or wind energy, or from nuclear energy (via direct thermal conversion or by electrolysis) and can be introduced into existing natural gas grids as a means of storage and distribution [46, 47].

Hydrogen is also one of the main components of synthesis gas (syngas) fuels than can be produced from renewable sources such as lignocellulosic biomass, or from fossil fuels such as coal or heavy oil. Due to the variety in the sources and the gasification processes, the composition of syngas fuels can vary widely. Syngas may contain H_2, CO, and CH_4, as well as CO_2, N_2, H_2O, and small amounts of higher hydrocarbons [19, 48]. Syngas can be used for power production using integrated gasification combined cycles (IGCC) [49]. In an IGCC, syngas is produced by gasification of lignocellulosic biomass or coal in the pressure range of 25 bar to 35 bar. In the case, that IGCC is combined with carbon capture and storage via pre-combustion CO_2 separation, most of the carbon monoxide is shifted to carbon dioxide, which is removed, from the syngas. As a result, the main constituents are hydrogen (> 80 % vol), nitrogen (about 10 % vol) and carbon monoxide (about 5 % vol) [50].

Combusting syngas or hydrogen-enriched natural gas in gas turbine combustors can affect the operability of the gas turbine combustors in several ways. Depending on the chemical and physical properties of the fuel mixture, gas turbine combustors can become prone to operability risks such as lean blowout (LBO), flashback (FB) and autoignition.

Fuel mixtures comprising H_2 have a particularly narrow operability range in lean premixed combustion. The high reactivity of H_2, manifests itself in a high flame propagation speed, and increases the risk of flashback even at very low equivalence ratios. If the flame speed is reduced by operating at very lean conditions, that may pose high risk of combustion instability and blowout.

Another issue that needs to be considered when using syngas or hydrogen-containing fuels are thermo-diffusive effects. The large differences in the diffusivity of various fuel and oxidizer components of such fuels may affect the local laminar flame speed and the flame resistance to strain. The thermo-diffusive effects can become more significant as the H_2 content of the fuel mixtures increases [51]. The thermo-diffusive effects can be expressed in terms of Lewis number which is defined as the ratio between the thermal and mass diffusivity [52].

2.4.2. Biogas

One of the most promising gaseous bio-fuels for gas turbines is digestion gas or 'biogas' [53]. Biogas is usually produced from anaerobic digestion of dung or sewage which yields CH_4 and CO_2 in varying concentrations as its major components. The inclusion of diluent species such as CO_2 or N_2 in the fuel mixture can affect the combustion properties of the mixture by changing the specific heat capacity and adiabatic flame temperature of the fuel [18]. It has been suggested in the literature that CO_2 dilution may also affect the combustion behavior by changing the chemical kinetic rates and radiative heat transfer [54]. Using biogas or other fuel mixtures that contain large fractions of diluents in gas turbines will result in lower flame temperatures and flame speeds and thus in a higher risk of blowout [54].

3. CHEMICAL KINETICS MODELING

Combustion in gas turbine combustors is controlled by the interaction of fluid mechanics, chemical kinetics and mass and heat transport. Developing fuel-flexible gas turbine combustors involves changing the reactants and their chemical kinetics. To study and understand the influence of chemical processes that are involved in a combustion system, simplified chemical reactor models may be used. Chemical reactor models are low-dimensional representations of chemically reacting flows. Although the fluid dynamic processes are simplified to a great extent in chemical reactor models, they can still be highly useful in modeling the combustion behavior under certain conditions. The most common reactor models used for gas turbine combustion are the perfectly stirred reactor (PSR), the batch reactor (BR) and the plug flow reactor (PFR) models. In some cases a network of these reactors can be used to produce a better approximation of the system. In this chapter a brief description of these models will be presented followed by a summary of the chemical kinetic modelling performed throughout this thesis.

3.1. Perfectly stirred reactor (PSR) model

A perfectly stirred reactor is an ideal reactor in which perfect mixing is achieved inside the control volume [9]. In a PSR model, all the transport properties are disregarded as it is assumed that turbulent and molecular mixing are much faster than chemical reactions. This means that in a PSR the combustion is controlled only by the chemical kinetics.

In a PSR, gases enter the reactor with a certain mass flow rate and composition and at a certain temperature. Upon entering the reactor, they mix instantaneously and perfectly with the gases that are already in the reactor. Thus, the composition and the temperature are uniform within the reactor. In a steady flow condition, the gases exit the reactor with the same mass flow rate as they entered and they will have the same temperature and composition as the gases inside the reactor [41]. The only parameter that can be used in a PSR model to consider different flow conditions is the residence time. The residence time in a PSR (τ_{PSR})

is defined as the time spent by the gases in the reactor and can be calculated as in Eq. (11),

$$\tau_{PSR} = \frac{\rho V}{\dot{m}} \tag{11}$$

where V is the volume of the reactor and $\dot{m}$ is the mass flow rate of the gases. The assumption of instantaneous perfect mixing is not true in most real combustion systems. Yet, in highly turbulent reacting flows where the turbulent mixing is much faster compared to the chemical reactions, the PSR model may be used. In swirl-stabilized combustors, very high levels of turbulence exist in the recirculation zone, which provides a fast mixing of the unburned and burned gases and promotes the spatial homogeneity. For simplified chemical kinetic studies, it is thus customary to model the chemical kinetics in the recirculation zone by a PSR model [41].

One of the chemical kinetic properties that can be estimated using a PSR model is the time scale of the reactions in the recirculation zone. The chemical time scale obtained from a PSR model can be used to correlate the lean blowout limits of various fuel compositions. This is done based on the assumption that the lean blowout occurs under the condition where the flow residence time is insufficient for the chemical reactions to take place.

Using a similar approach, the PSR model can be used to correlate flashback limits when the flashback is driven by combustion induced vortex breakdown (CIVB). In the case of CIVB flashback, the interaction with the flame causes the recirculation zone to move into the premixing section with the flame tip being attached to the stagnation point. Further flame propagation into the premixing section depends on the competition between the heat release from the flame and the local flame extinction because of the high turbulent mixing in the recirculating bubble [21, 55]. The chemical time scale obtained from a PSR model can be used as a measure of the chemical reaction time. A comparison between the chemical time and the flow residence time in the recirculating bubble may be used to correlate CIVB flashback limits for a given combustor geometry [56].

3.2. Batch reactor model

A batch reactor model is an ideal closed homogenous reactor which is characterized by a fixed amount of mass. The gases in a batch reactor are assumed to be perfectly mixed with no mass flow in or out of the reactor. The reactor is usually defined as a constant volume or constant pressure system. Batch reactor models can be used to determine the ignition delays of various fuel/oxidizer mixtures under a specified set of initial pressure and temperature conditions [9].

3.3. Plug-flow reactor (PFR) model

An ideal plug-flow reactor is a one dimensional continuous steady flow of reacting gases in a channel or a duct. The composition and temperature can vary along the length of the reactor (axial direction) but there is no variation across the reactor [41]. This means that ideal plug-flow reactors are radially uniform in their velocity profile and species concentrations. In addition, in an ideal plug-flow reactor mixing and diffusive transport along the length of the reactor is disregarded. The time spent by the reactant in the reactor is the ratio of the axial location of the reactants in the reactor and their axial velocity. In a real flow reactor, some portion of the reactants may spend a longer time in the reactor due to the existence of recirculation zones or a large boundary layer.

In premixed gas turbines, the fuel/air mixture spends a finite time in the premixing section under turbulent conditions and at elevated temperatures and pressures, which can be mimicked using experimental flow reactor facilities. Since the pressure is nearly constant, and by disregarding the radial and axial transport the ignition, delays may be estimated using a plug-flow reactor model. However, in real gas turbine combustors, mixing of the reactants occurs after fuel injection and by turbulent mixing and diffusion of species in all directions. The axial velocity may vary in radial direction and surface reactions and heat transfer may take place at the reactor walls. All of these conditions represent violations of ideal plug-flow assumptions. Despite the non-ideal conditions in real flow reactors, experimental studies in flow reactors have shown that plug-flow reactor models can provide reasonable agreement between experiments and modelling for a wide range of conditions.

3.4. Chemical kinetic modeling in the current work

An objective of this thesis was to compare the experimental results to chemical kinetic calculations and to investigate the usefulness of these simplified models in predicting the lean blowout, flashback and autoigniton experimental results. The following sections present a brief summary of the chemical kinetic modeling conducted for lean blowout, flashback and autoigniton.

3.4.1. Lean blowout

A PSR model was used to predict the experimentally measured lean blowout limits presented in Paper **I** and Paper **II**. The comparison between the experimental values and the model predictions is given in Papers **I** and Paper **II**. Generally speaking,

21

although the PSR model predicted some of the trends observed in the experiments, it was unable to accurately predict the lean blowout limits in the variable-swirl combustor.

3.4.2. Flashback

A PSR model was used to estimate the chemical time scale of various fuel mixtures at their experimentally obtained flashback equivalence ratios. This was done as an attempt to correlate the measured flashback limits with a quench constant as proposed by Kröner et al. [56]. According to the work of Kröner et al., in the case of CIVB flashback, the flashback limits of a combustor with a given geometry may be correlated with a critical quench constant. The quench constant is defined as the ratio between a chemical time scale at flashback equivalence ratio and a flow time scale of the recirculating bubble as presented in Eq. (12).

$$C^*_{quench} = Le_F . \tau_{PSR} . \frac{U_b}{D} \tag{12}$$

Where τ_{PSR} is the residence time of a PSR at the measured flashback equivalence ratio, U_b is the bulk velocity in the premixing section, D is the diameter of the premixing section and Le_F is the lewis number of the fuel. The Lewis number was added to the definition of quench constant to account for the preferential diffusion effect which is important in hydrogen containing fuels. Using Eq. (12), the quench constant was calculated for the flashback limits that are presented in Paper **IV**. It was observed that the quench constant correlated with some of the experimental results. However, the experimental data set was not sufficiently large to conclude the validity of this criterion.

3.4.3. Autoignition

The ignition delays of the tested fuel/air mixtures were calculated using batch reactor and plug-flow reactor models. The calculations were conducted in Chemkin software package [57] using chemical kinetic mechanisms available in the literature. The comparison of the model calculations using different mechanisms and the experimental results are presented in Paper **VI** and Paper **VII**. In addition to ignition delay calculations, a reactor network model was developed to estimate the error that was introduced to the measured ignition delays due to the fintie mixing time of the reactants in the flow reactor. This approach is described in detail in the following sub-section.

Mixing error estimation

In a simple PFR model it is assumed that the inlet flow to the reactor is a homogeous mixture of fuel and air which starts reacting upon entering the reactor.In reality, the air and fuel take a certain time to completely mix and reach the global equivalence ratio. This will create fuel-rich and fuel-lean zones in the fuel and air streams which start reacting at higher and lower equivalence ratios than the average value. This introduces a source of error in the measured ignition delays with respect to the ideal case of a simple PFR model. A reactor network model was developed to estimate this mixing error in the measured ignition delays. The reactor network consisted of two transient perfectly stirred reactors whose outlet flows merge and enter a plug-flow reactor. The PSRs were used to take into account the reactions occurring in the fuel-lean and fuel-rich streams prior to complete mixing. During the mixing time, the equivalence ratio of the air-side stream increased from zero to the target equivalence ratio. Similarly, the equivalence ratio of the fuel-side stream decreased from infinity to the target equivalence ratio. During this process, reactions took place in both PSRs. When the target equivalence ratio was reached, the chemical composition of the exit flow of the two PSRs was mixed, and was assumed to correspond to the composition entering the PFR. The time necessary for the fuel and air to fully mix and reach the target equivalence ratio was estimated experimentally using an FID probe, as described in Paper **VI**. The measured mixing time is used in the model as the transient time of the PSRs. By knowing the transient time and the final equivalence ratio, the required residence time of each PSR can be calculated based on the transient mass balance in the PSRs as given in Eq. (15) and Eq. (16).

$$\frac{dY}{dt} = (\frac{1}{\tau_{res}})(1 - Y) \tag{13}$$

$$\tau_{res} = -\frac{\tau_{transient}}{\ln(1 - Y)} \tag{14}$$

where $\tau_{transient}$ is the transient time of the PSRs and is equal to the measured fuel and air mixing time. τ_{res} is the required residence time of the PSR and Y is the fuel mass fraction for the lean PSR and air mass fraction for the rich PSR which can be calculated based on the final equivalence ratio.

Using this model, the ignition delay of a given mixture will be the sum of the mixing time and the PFR ignition delay. In this way, the history of the reactions and temperature during the mixing time is taken into account in the inlet flow of the PFR and hence influences the ignition delay of the PFR model. By comparing the results of the reactor network model with a simple PFR model the mixing error can be calculated for various conditions. More details on the mixing error estimation can be found in the supplementary material of Paper **VI**.

24

4. EXPERIMENTAL SETUPS

Two experimental facilities were designed and built at the Division of Thermal Power Engineering, Lund University to investigate lean blowout, flashback and autoignition in premixed combustion using alternative fuels: First, an atmospheric premixed variable-swirl combustor to study lean blowout and flashback of various fuel mixtures at different operating conditions. Second, a pressurized turbulent flow reactor to study autoignition of various fuel/air mixtures at varying temperatures and pressures. In this chapter, these two experimental facilities will be described.

4.1. Variable-swirl combustor

The atmospheric premixed variable-swirl combustor was used to investigate the lean blowout and flashback of gaseous fuel/air mixtures under different operating conditions. The swirl number in the combustor was varied between $S = 0.00$ to 0.66. By varying the swirl number, different flow fields were created in the combustor that made it possible to study the interaction of flow field and chemistry in combustion of various fuel/air mixtures. Two versions of the variable-swirl combustor were used throughout this thesis. The first version was used to study lean blowout of various biogas and syngas mixtures (Paper **I** and **II**). The combustor was then modified to enable visual investigation of flame flashback using an optical premixing section (Paper **III** and **IV**).

4.1.1. Variable-swirl combustor: version I

As illustrated in Figure 2, the combustion chamber consisted of a quartz tube, 63 mm in diameter, 350 mm in length, with a wall thickness of 3.4 mm. The combustor was supplied with swirling flow of fuel and air, through a centrally located premixing section, 15 mm in diameter and 30 mm in length. A swirl mixer (Figure 3), was, used to combine axial and tangential airflows coming from an axial inlet tube and a radial swirler surrounding the inlet tube. The swirl mixer was located at the entrance to the premixing section, and allowed for the introduction of air into the premixing section in axial and tangential directions in varying proportions.
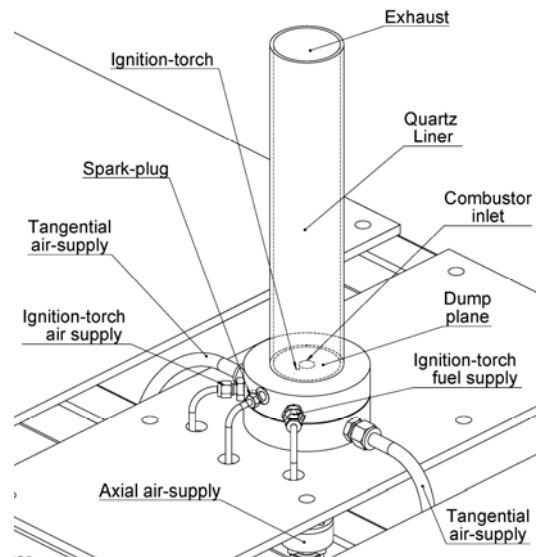
Figure 2.
Schematic of the variable-swirl combustor version I [58].

The geometry of the combustor is shown in Figure 3. The flow entering the swirl mixer in axial direction was premixed with fuel 250 mm upstream of the inlet tube, and passed through a fine wire mesh. The flow entering the swirler in the tangential direction passed through four channels that were 3 mm wide and 10 mm high. The swirl number of the flow entering the combustor was varied by changing the proportion of tangential to axial flow through the swirler. Axial and tangential flows were controlled and metered using two laminar-flow, differential-pressure mass flow controllers (Alicat MCR250). They were preheated individually using two feedback-controlled air heaters (Sylvania Sureheat Jet) of 8 kW power. General specifications of the combustor are presented in Table 1.

Table 1.
General specifications of the variable-swirl combustor

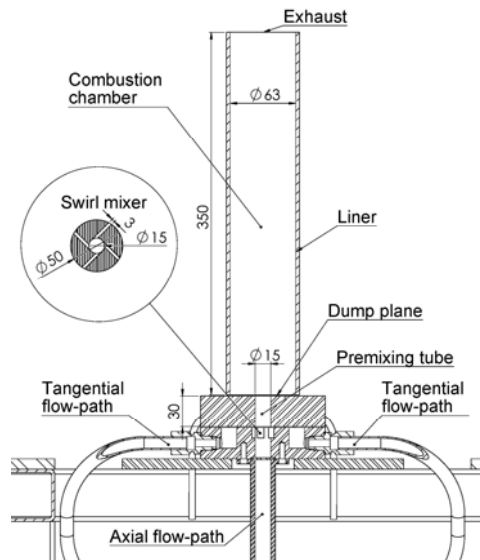| Volume [m^3]	0.0019	Reynolds number (preheated)	27000
Inlet temperature [K]	298-650	Reynolds number (cold)	42000
Pressure [atm]	1.00	Maximum thermal power [kW]	27.50
Air mass flow rate [SLPM]	50-500	Maximum combustion intensity [$MW.atm^{-1}.m^{-3}$]	25.20
Maximum inlet velocity [m/s]	46.00	Maximum combustor loading [$kg.s^{-1}.atm^{-1.8}m^{-3}$]	4.00

26

Figure 3.
The geometry and flow paths for axial and tangential flows for the variable-swirl combustor version I [58].
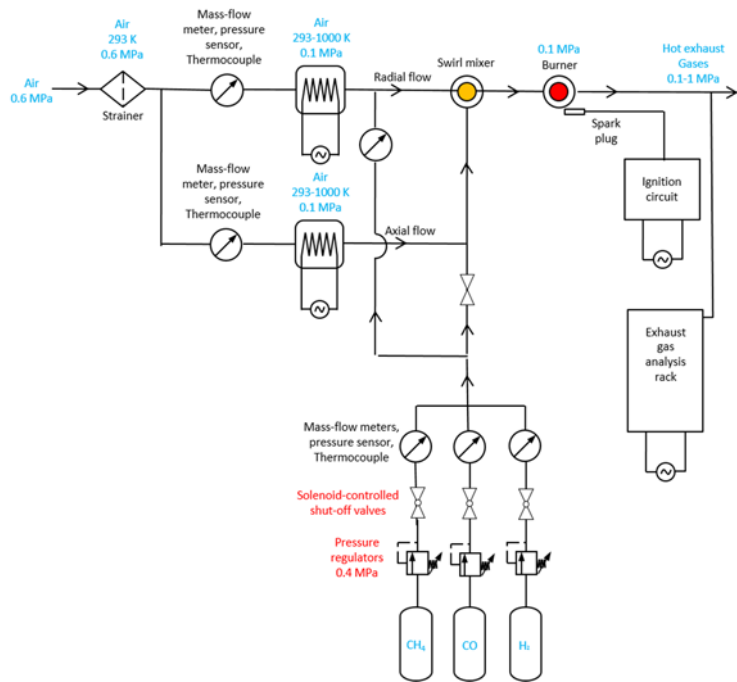

Figure 4.
The layout of the experimental setup used with variable-swirl combustor version I.

Fuel blends of desired compositions were generated by mixing the flows generated by three laminar-flow differential-pressure mass flow controllers (Alicat MCR50) supplying H_2, CO and CH_4 (purity 99.98 %) from gas bottles. The fuel gases were mixed with the axial air flow 250 mm upstream of the swirler. After passing through the premixing section, the premixed fuel and air mixure entered the combustion chamber through a sudden expansion step, referred to as the dump-plane.The combustion chamber discharged the flow directly into a force-ventilated extractor hood open to the laboratory air. The layout of the combustor together with the mass flow meters and air heaters is shown in Figure 4.

4.1.2. Variable-swirl combustor: version II

The main reason for modifying the original variable-swirl combustor was to enable visualization of flame flashback in to the premixing section by means of an optical premixing section. An overview of the second version of the variable-swirl combustor can be seen in Figure 5. In the modified version of the combustor, the diameter and the overall length of the combustor were similar to those of the original version. However in the modified version, only the first 120 mm of the combustor consisted of a quartz tube which provided optical access to the combustor.

In addition, the premixing section in the modified version was extended using a quartz premixing section of 50 mm length and 15 mm diameter directly upstream of the combustor. Using an optical premixing section directly upstream of the combustor allowed for detection and visualization of flame flashback from the combustor to the premixing section. Another modification made in the second version of the combustor was to use an additional laminar-flow, differential-pressure mass flow controller (Alicat MCR50) 240 mm upstream of the swirler to split and control the fuel flow between the axial and tangential air flows based on their mass flow rates. This was done to ensure that the equivalence ratio of the fuel/air mixture entering the combustor was the same in both axial and tangential directions. A schematic of the combustor cross-section and the details of the geometry are shown in Figure 5 and Figure 6.
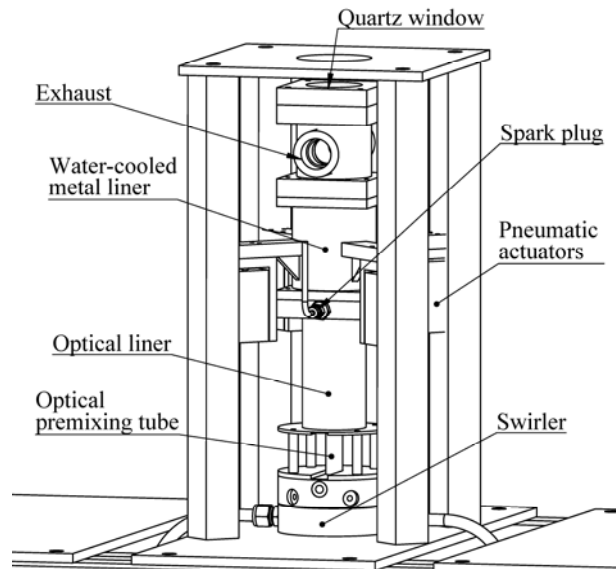
28

Figure 5.
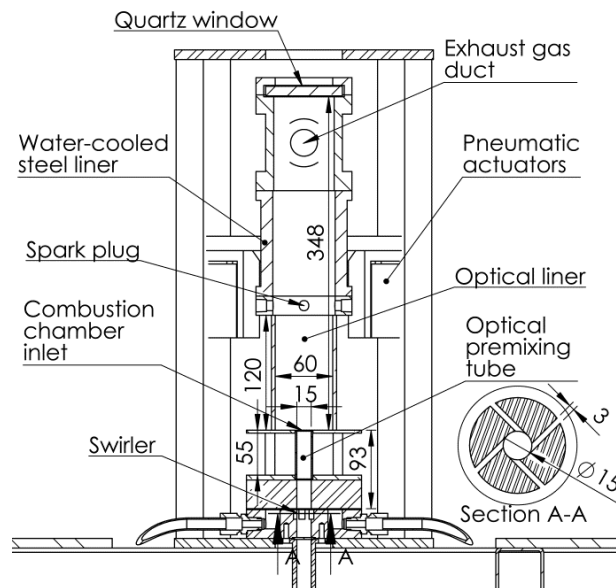The schematic of the variable-swirl combustor version II [24].

Figure 6.
The geometry of the variable-swirl combustor version II [24].

4.2. Turbulent flow reactor

The pressurized turbulent flow reactor that was used for autoignition studies, featured an optically accessible test section which allowed for visual investigation of autoignition flames. An overview of the flow reactor is presented in Figure 7.

The flow reactor consisted of an air supply system, a fuel supply system, a pipe of circular cross section and an exhaust system. Different parts of the flow reactor will be described in the following sections.

4.2.1. Air supply system

The air was supplied to the system by means of a screw compressor (Ceccato CSB 25-13) with a supply pressure of 1.3 MPa and a mass flow capacity of 45 g/s. An air-cooler (BIAB DE025) was used to dry the air before entering a steel pressure vessel. The pressure vessel had a volume of 0.5 m^3. Depending on the desired pressure in the flow reactor, a certain amount of air was bled off the pressure vessel using an automatically-controlled, pneumatically-actuated sliding gate valve (Schubert & Salzer 8020). The air mass flow to the flow reactor was measured by means of a Coriolis mass flow meter (Micromotion). Before entering the flow reactor the air was passed through a non-return valve and a tubular air heater of 27 kW power [59].
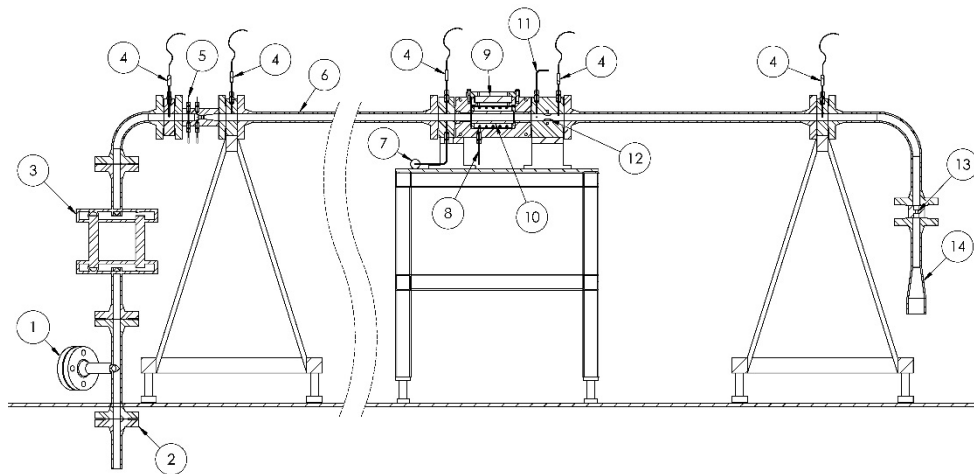

Figure 7.
Flow reactor schematic. 1) Air inlet from compressor 2) Safety burst disc 3) Electric air heater 4) Thermocouples 5) Fuel injector 6) Ignition delay section 7) Pressure transducer 8) Cooling air for outer quartz windows 9) Outer quartz windows 10) Inner quartz tube 11) Water injector 12) Air dilution 13) Throttling valve 14) Exhaust duct [59].

30

4.2.2. Fuel supply system

The fuel was injected and mixed with the incoming air flow using a venturi tube which was located at the beginning of the flow reactor. The Venturi tube constricted the diameter of the tube from 23.7 mm to 11.85 mm. Fuel flow was introduced to the venturi tube through one centrally located axial fuel jet ahead of the venturi tube and four radially inward pointing jets ($\varnothing$ = 1 mm) located in the converging section of the venturi tube. A cross-section schematic of the fuel injection arrangement is shown in Figure 8 [59].
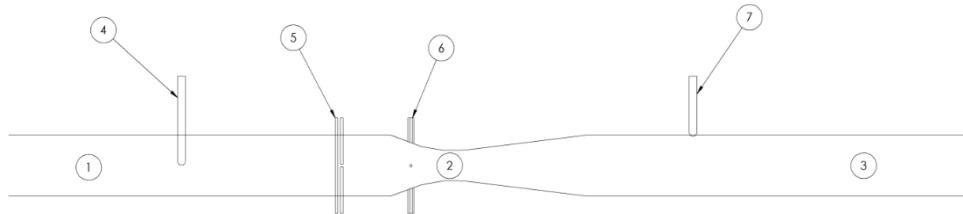

Figure 8.
Section schematic of venturi tube fuel-injector. 1) Air inlet 2) Venturi tube 3) Reactor 4) Centrally located thermocouple at air inlet 5) Fuel supply to centrally located axial injector 6) Fuel supply to four radially inward pointing injectors 7) Wall mounted thermocouple in reactor [59].

4.2.3. Test section

The test section of the flow reactor consisted of a pipe with a circular cross section. The overall length of the test section was 4.47 m including the venturi tube. The internal diameter of the pipe cross section was 23.7 mm. To provide optical access to the test section, 135 mm of the test section consisted of a quartz glass tube with a wall thickness of 2.5 mm. The quartz tube was located at the end of the test section, within an optically accessible pressurized chamber and was surrounded by cool purging-air at approximately the same pressure as that inside the quartz tube. The optically accessible chamber had three quartz windows of 100 mm length, 30 mm height and 20 mm thickness, through which the inner quartz tube could be viewed. Apart from the quartz tube and windows, the material of the test section was austenitic alloyed steel (AISI 253 MA, EN 1.4835). The temperature along the test section was measured using several Chromel-Alumel (K-type) thermocouples. A diaphragm pressure sensor (Tecsis E113) was located at a distance of 69 mm upstream of the quartz tube to measure the static pressure within the test section. For some of the experiments the test section was heated using feedback-controlled electric resistance heaters.

A photoelectric cell (Hamamatsu UVtron R9454) sensing the emission of ultraviolet light (UV) was used to detect the presence of UV-radiation (wavelength

31

sensitivity 185-260 nm) from the autoignition flames through the top window of the optically accessible section of the flow reactor [59].

4.2.4. Exhaust system

After flowing through the test-section, the gases were quenched using a water jet injected into the gases. This was done by means of a hydraulically-actuated diaphragm dosing pump (Milton Roy Dosapro). In this manner, the gases were cooled to a temperature between 500 and 600 K before being expanded through an automatically-controlled pneumatically-actuated sliding-gate valve (Schubert & Salzer 8020) [59].

5. MEASUREMENT TECHNIQUES

Several experimental techniques were used in this thesis to investigate the combustion of alternative fuels under different conditions. Apart from the basic temperature, mass flow and pressure measurements that were performed to quantify the experimental conditions, more advanced velocity measurements and visualization techniques were employed to provide a deeper understanding of the studied phenomena. The flow field in the combustor was studied using laser-based velocity measurement methods such as LDA and PIV. The flame structure was visualized using natural luminosity imaging as well as high-speed OH*-chemiluminescence imaging. In the lean blowout experiments, CO emission measurements were performed to confirm the proximity to lean blowout limit for various fuel mixtures. In this chapter some of these experimental methods will be described briefly.

5.1. Laser Doppler anemometry (LDA)

LDA is a laser-based technique which is used for measurements of local fluid velocities and their fluctuations. LDA is considered as a non-intrusive technique which can provide time-resolved velocity measurements. In this method, particles of certain size and density will be introduced into the flow assuming that they will follow the fluid motion. In a two-component arrangement, the velocity of a moving particle is measured in the intersection of two laser beams. The basic principle of LDA can be explained using two different approaches namely Doppler shift approach and fringe model approach. Short descriptions of these approaches will be presented in the following sections. A more detailed description of the LDA technique can be found in [60-62].

5.1.1. Doppler Effect

The Doppler effect in optics refers to the frequency shift of the light wave when the light source is moving or the light is reflected off a moving surface. The LDA technique is based on the detection of this frequency shift in the scattered light from a moving particle which has been illuminated by a laser light. By knowing the

frequency shift (Doppler shift) in the scattered light, the velocity of the particle can be calculated. However, even at very high particle velocities, the frequency of the scattered light is in the order of the frequency of the light source and therefore too high to be measured by conventional devices that are found in usual laboratories. For this reason a dual beam arrangement is used in the LDA technique [60].

In a dual arrangement, two laser beams of equal frequencies illuminate the particle, resulting in two scattered waves whose frequencies are shifted differently by the Doppler Effect. A photo detector is usually used to receive the scattered light from the illuminated particle. The two scattered light waves received by the detector are superimposed. The output of the photo detector has the following form:

$$(sin \, \omega_1 t + sin \, \omega_2 t)^2 = \, sin^2 \, \omega_1 t + sin^2 \, \omega_2 t + 2sin \, \omega_1 t \times sin \, \omega_2 t \qquad (15)$$

where ω_1 and ω_2 are the frequencies of the two scattered light waves. The frequency of the squared term is too high to be resolved by the detector, but the cross product can be rewritten as:

$$2sin \, \omega_1 t \times sin \, \omega_2 t = \, cos(\, \omega_1 + \, \omega_2)t + cos(\, \omega_1 - \, \omega_2)t \qquad (16)$$

Thus the output will exhibit a low frequency of (ω_1- ω_2), which can be easily measured by conventional measurement devices. This low frequency is called Doppler frequency in the terminology of LDA measurement technique. The Doppler frequency is directly proportional to the velocity component of the particle that is perpendicular to the bisector of the two laser beams and is independent of the particle motion direction as presented in Eq. (17). The flow velocity can hence be obtained by measuring the Doppler frequency assuming that the particle moves with the same velocity as the flow.

$$u_\perp = \frac{\lambda_0}{2sin\alpha} \, \omega_D \qquad (17)$$

where λ_0 is the wave length of the light source, ω_D is the Doppler frequency and α is the half angle between the two laser beams as illustrated in Figure 9.
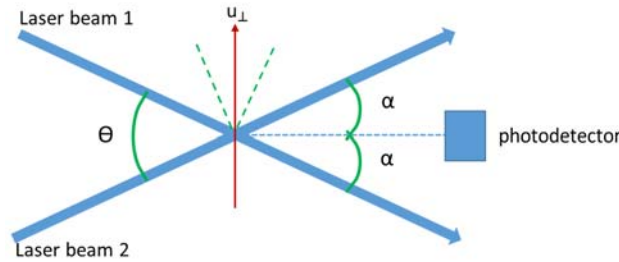

Figure 9.
Particle motion through the measurement volume in LDA.

5.1.2. Fringe model

The fringe model is considered as a simpler approach for explaining the LDA principles compared to the Doppler shift approach. It is based on the interference of two laser beams that intersect in a measurement volume. Due to the coherent properties of laser light, the intersection of two laser beams creates an interference pattern as the light waves cancel each other in some regions and complement each other in other regions. This results in alternating dark and bright planes, known as fringes, in the intersection of the beams. When a light-scattering particle travels through the intersection of the two laser beams, it scatters a periodic light flux. The reflected light is collected and transformed to an electrical current usually by means of a photo multiplier. The signal from the photo multiplier is called the burst signal as shown in Figure 10. The low frequency component of the burst signal is called the pedestal which is due to the Gaussian intensity distribution of the laser light in the measurement volume. The high frequency of the burst signal is the Doppler frequency and is proportional to the particle velocity component that is perpendicular to the direction of the fringes. This velocity component can be obtained by multiplying the fringe spacing, d_f, with the Doppler frequency, ω_D, which is the number of fringes traversed per unit time [60]:

$$u_\perp = \omega_D d_f \tag{18}$$

The fringe spacing is only dependent on the wavelength of the laser light, λ_0, and the intersection half-angle of the beams, α, and can be calculated as follows:

$$d_f = \frac{\lambda_0}{2 sin\alpha} \tag{19}$$

With the basic LDA technique described above, the direction of the flow cannot be determined because a positive and a negative velocity of the same magnitude will result in the same Doppler frequency. In order to obtain the flow direction from the Doppler burst signal, one of the laser beams is frequency-shifted using a Bragg cell. This results in a movement of the fringes in the measurement volume with the frequency of the shift frequency. In this manner, a zero velocity will correspond to the shift frequency and the flow direction relative to the fringe movement can easily be determined.

The scattered light from the moving particles can be detected by separate optics (off-axis detection) or using the emitting optics (backscatter). The simplest setup is to use the optics in backscatter mode in which the emitting and receiving optics are integrated into one unit. The Doppler frequency is usually determined using Fourier transform or correlation techniques which have the ability to extract the Doppler frequency even at low signal to noise ratios. Since the particles arrive at the measurement volume at different times, special triggers must be used to start the measurements. One of the available commercial analyzers that is built for LDA, is the Burst Spectrum Analyzer (BSA) from Dantec. The schematic of a backscatter

LDA system is shown in Figure 10. The spatial resolution of the LDA measurement is dependent on the measurement volume size. The geometric measurement volume which corresponds to the point of intersection of the two laser beam has a diamond-like shape. Since the laser beams has a Gaussian intensity distribution, the effective measurement volume becomes ellipsoidal. The length, l_m, and the diameter, d_m, of the measurement volume at the e^{-2} limit can be calculated based on Eq.(20) and Eq. (21) respectively.

$$l_m = \frac{4\lambda_0 f}{D_{e^{-2}} \sin\alpha} \tag{20}$$

$$d_m = \frac{4\lambda_0 f}{D_{e^{-2}} \cos\alpha} \tag{21}$$

where λ_0 is the wave length of the laser light, f is the focal length of the focusing lens used to make the two laser beams intersect, $D_{e^{-2}}$ is the diameter of the beams at the e^{-2} limit before the focusing lens and α is the intersection half-angle. It is noted that the measurement volume should always be created by arranging the intersection of the two beams on their waists respectively. The measurement volume size has a strong influence on the quality of flow measurements when using the LDA technique. Moreover, in order to have an accurate evaluation of the velocity, a minimum number of fringes must be passed by the particle. The size of the particle and whether it passes through the center of the measurement volume or not, also influence the detected signal.

The particles that are used in LDA measurements as seeding must have the proper size, shape and density. Moreover, the concentration of the particles must be sufficiently high and they should be uniformly distributed in the flow. In an LDA system in backscatter mode the refractive index of the particles play an important role in obtaining high signal quality.
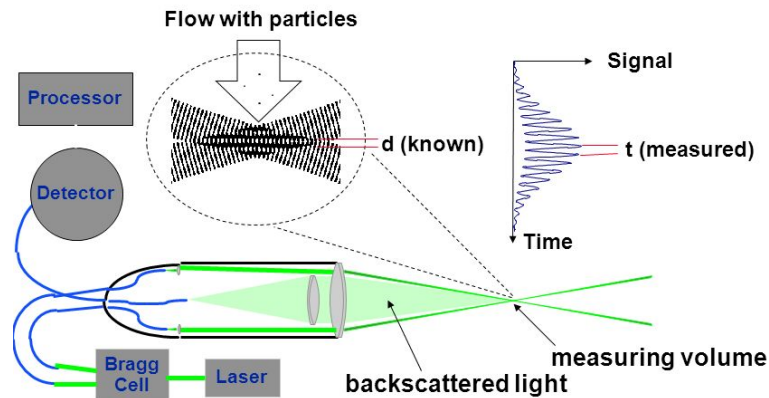

Figure 10.
The schematic of a back-scatter LDA system, Dantec Dynamics [63].

36

5.1.3. The LDA system used for the current work

The LDA technique was used in this thesis to determine the swirl number of the flow at the inlet of the combustor for different axial/tangential mass flow ratios. The axial and tangential velocity profiles were measured 1 mm above the dump plane of the combustor. The LDA system was a two-component, optical-fiber-based LDA system (Dantec) operated in backscatter mode. The light source consisted of an Argon ion laser (Spectra Physics) operated between 1 and 2 W power output (all lines). Beam expansion (1.94 times) was used before the front lens (310 mm focal length) to reduce the size of the measuring volume to approximately 50 μm in diameter and 500 μm in length. Signal processing was performed using two burst spectrum analyzers (Dantec).

During the LDA measurements, a length of 100 mm of the quartz liner was replaced with a stainless steel liner of a similar diameter, but with two flat windows located on opposite sides to allow the laser light to enter and exit the combustion chamber with reduced light refraction losses. The overall length of the liner was 350 mm, as in the combustion experiments. The cross-sectional geometry of this altered section is shown in Figure 11.
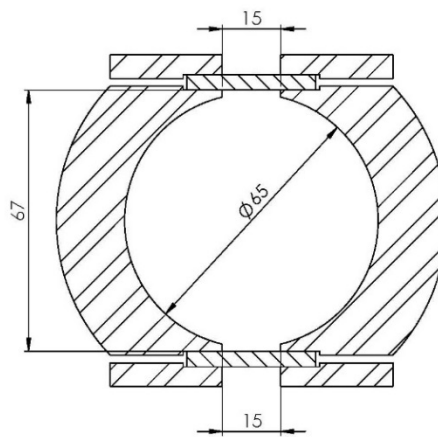

Figure 11.
Cross-section of the liner used during the LDA measurements.

In order to measure the velocity as close as possible to the dump plane of the combustor, the probe was tilted by 7 degrees. Using a tilted probe had no impact on the tangential velocities, but the axial velocities should ideally be corrected for the probe angle and radial velocity component at each measuring position. However, due to the limited optical access of the liner preventing the radial velocities from being measured, the radial velocities were measured for the highest and lowest swirl cases without the liner and as expected, they were an order of magnitude smaller than the axial and tangential velocities. Since the probe tilting angle was also very

small; the effect of the radial velocity component on the axial velocity was neglected which introduced an additional relative error of 2.5% to the axial velocity measurements. In addition, a transit-time velocity bias correction was made to the measured velocities, but the difference was < 2% at all points. The relative errors due to determination of calibration factor (fringe distance), finite number of samples and positioning the measuring volume were estimated to be 1.5 %, 0.2%, and 1%, respectively. Hence, the total relative error in the velocity measurement was estimated to be 4%.

The LAD measurements were conducted at the ambient temperature (298 K). This allowed reducing health risks by seeding the flow with liquid droplets consisting of a mixture of glycols and deionized water, instead of the metal-oxide particles that would have been required for measurements at high-temperature. The droplets were created using a six-jet air-driven atomizer (TSI) and the air added through the seeder was metered using a thermal mass flow meter (Bronckhorst F-112AC). The number mean droplet diameter generated by the seeder was 0.35 μm. The seeded flow was added to the tangential air flow except in the cases of very low swirl numbers, in which the seeded flow was added to the axial flow [58].

5.2. Particle image velocimetry (PIV)

PIV is a laser-based technique which provides simultaneous velocity measurements at several points in a plane of a flow. A detailed discussion of the PIV technique can be found in [64], but its basic principle will be explained briefly in the following paragraphs.

In a two dimensional PIV measurement, two laser pulses from one or two Nd:YAG laser are expanded into 2-D laser sheets by means of a cylindrical lens. The two successive pulses illuminate the particles following the flow in the plane of the light sheet. The laser pulses are synchronized to a CCD camera that is arranged perpendicular to the laser sheet plane. After each pulse, the light scattered from the particles due to Mie scattering is recorded as a single CCD image frame. The schematic of a PIV system is shown in Figure 12.
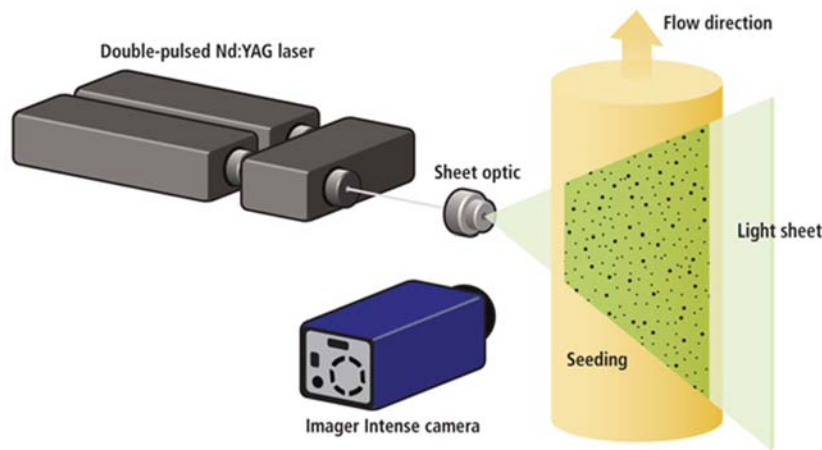
Figure 12.
The schematic of a 2-D PIV system, LaVision [65].

The images are divided into a grid of interrogation areas. By comparing the images recorded from the two successive laser pulses, the displacement of the visual patterns from its initial interrogation area can be estimated. Since the time delay between the pulses is known, velocity can be determined as the ratio of the visual pattern displacement and time between the pulses.

The thickness of the laser sheets is chosen based on the flow velocity that is perpendicular to the laser sheet, which is referred to as out-of-plane velocity. The time delay between the pulses is chosen based on the flow characteristics: large enough to have a noticeable displacement of the visual patterns and small enough to avoid loss of patterns between the two images mainly due to the out-of-plane particle motion. The particles that are introduced into the flow for PIV measurements should on one hand have sufficiently small size to be able to follow the flow and on the other hand be large enough to scatter sufficient light. Moreover, the particles should be homogenously distributed in the flow to ensure reliable velocity determination in the entire domain of interest.

The size of interrogation areas is chosen based on the expected velocities and the particle density in the flow. The displacement of particles between the two pulses should be approximately 1/4 of the size of each interrogation area. In this work, the interrogation areas typically consisted of 32 x 32 or 64 x 64 pixels. Each interrogation area produces a velocity vector. This velocity vector is usually found using mathematical correlation between interrogation areas of the two successive frames. If the images from the two pulses are recorded in two separate frames, the velocity vector is found using a cross-correlation technique. This means that each interrogation area in the second frame is shifted in all directions to find the best match with the respective interrogation area in the first frame. In the case where the images from the two pulses are recorded in one single image, auto-correlation is

used to find the velocity vector for each interrogation area. The cross-correlation can be expressed as Eq. (22).

$$R(s) = \int_{A_I} I_1(x) I_2(x + s) dx \tag{22}$$

where s is a two-dimensional displacement vector, A_I is the interrogation area and $I_1(x)$ and $I_2(x)$ are light intensities in the interrogation area of the first and second frames, respectively. The peak of $R(s)$ corresponds to the best match with s being the displacement vector. Validation of the velocity vectors is done by requiring a minimum ratio between the two highest cross-correlation peaks (Figure 13).

It should be noted that the obtained velocity vector of each interrogation area corresponds to the average velocity of all particles in the interrogation area obtained in the time between the two pulses. This means that in order to have a robust measurement a sufficient number of particle pairs must be present in each interrogation area.

There are several algorithms available for enhancement of the correlation and better determination of the velocities. By using multi-pass schemes, displacement and deformation of the second interrogation area with respect to the first interrogation area can be estimated and used to increase the correlation. In a multi-pass scheme, the size of the interrogation area is reduced in an iterative process. The results from the larger interrogation areas are used as 'pre-displacement' for smaller interrogation areas [66]. Another way to increase the correlation and the spatial resolution of the measurements is to overlap the interrogation areas to find the best displacement match. Using a standard PIV algorithm the displacement of particles can be estimated within an accuracy of 1/2 pixel. The need for higher accuracy has produced several peak-finding algorithms that can estimate the peak location to sub-pixel levels [67]. There are also algorithms available to reduce errors that can be introduced if the scattered light from the particles occupy less than a pixel on the CCD image. This causes the calculated displacements to be biased towards integer values because the position of the particle will be estimated at the center of the pixel. This error which is referred to as 'peak locking error' can be reduced using sub-pixel interpolation methods [68].
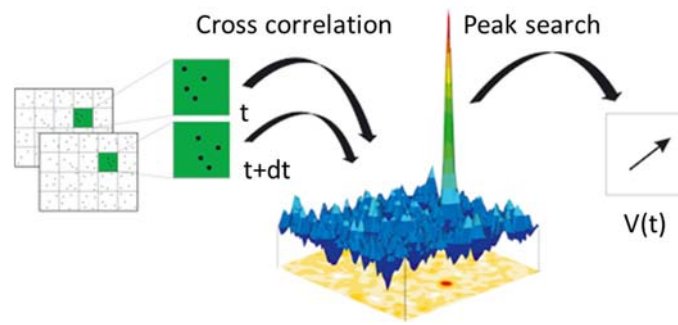
Figure 13.
Using cross correlation in evaluation of PIV recordings [65].

5.2.1. The PIV system used in the current work

The flow field in the combustor was measured using a high-speed PIV system (Lavision Flowmaster) with a wavelength of 527 nm and at a frequency of 2.5 kHz. A diode-pumped, dual cavity Nd:YLF laser (Litron LDY) was used to illuminated the central plane of the combustor at a sheet thickness of approximately 1 mm, using a diverging light sheet generated by an optical lens. The pulses had a time delay of 27.5 μs. The laser light scattered off the TiO_2 seeding particles and was recorded at a repetition rate of 2.5 kHz with a resolution of 512 x 800 pixels and a depth of 12 bit using a high-speed CMOS camera (Vision Research Phantom V 611). The TiO_2 particles were seeded into the flow using a rotating-drum particle seeder (Scitek PS-10). Velocity fields were evaluated from particle images using a multi-pass cross-correlation algorithm available in the DaVis (v. 8.1.4) computer software. The cross-correlation was performed on interrogation areas of 64 x 64 and subsequently 32 x 32 pixels with a window overlap of 50 %. The time-averaged velocity fields were obtained by averaging over 2500 instantaneous vector fields, which was equivalent to a time interval of 1 s. The details of the analysis algorithms can be found in the product manual of DaVis 8.1 [65]. It should be noted that due to the interaction between the laser light and the glass combustor liner, fixed patterns were present in the raw PIV images which made it problematic and for some cases impossible to obtain velocity vectors in those areas of the flow field [69].

5.3. High-speed OH*-chemiluminescence imaging

Optical emissions from the flame can be used to study the structure of the flame under different conditions. One of the sources of light emissions from the flame is chemiluminescence. Chemiluninescence is the electromagnetic radiation emitted

41

from the de-excitation of electronically excited species that are formed via chemical reactions in the combustion reaction zone. In typical hydrocarbon flames, most of the visible and ultraviolet chemiluminescence radiation is emitted from radicals such as CH^*, OH^*, C_2^* and CO_2^*. Studying the chemiluminescence from these radicals can thus provide information about conditions in the reaction zone, flame position, shape and structure of the flame in combustors [70].

In this thesis, high-speed OH^*-chemiluminescence imaging was used in flashback and autoignition experiments. In the flashback experiments, OH^*-chemiluminescence imaging was used to visualize the occurrence of the flashback and unsteady propagation of the flame in the premixing section [24, 69]. In the autoignition experiments, OH^*-chemiluminescence imaging was used to visualize the occurrence of autoignition and study the spatial and temporal development of autoignition kernels for various fuel/air mixtures [59, 71].

The OH^*-chemiluminescence imaging was done using a high-speed camera (Vision Research Phantom V 611) equipped with an image intensifier (Hamamatsu C4598), a band-pass filter (Acton Research 310.5±5.75nm) and a phosphate glass lens (UV-Nikkor 105 mm, f/4.5) to photograph OH^*-chemiluminescence of the flame around 306 nm at high-speed. OH^*-chemiluminescence images were recorded at a resolution of 512×512 pixels and a frame rate of 13550 frames per second. Each frame had an exposure time of 72 μs. The images were corrected for background noise and calibrated spatially to the dimensions of the combustor. To improve the visual clarity, the intensity of the images was altered for each individual test condition. In flashback experiments, in order to estimate the flame front position in the optical section of the premixing section, the images were individually thresholded and the flame front boundaries were approximated based on the gradient of the pixel counts in the image.

5.4. CO emission measurements

CO emission measurements can be used to detect operational proximity to the lean blowout limit when using fuel mixtures containing hydrocarbons or carbon monoxide. When combusting such fuels, CO can be one of the combustion products under fuel-lean as well as fuel-rich conditions.

When the combustion is fuel-rich, production of CO occurs due to the lack of oxygen, which leads to incomplete reaction of hydrocarbons with O_2. At stoichiometric or slightly fuel-lean condition, production of CO is the result of dissociation of CO_2, which is linked to the high temperature of the flame. Reducing the equivalence ratio towards leaner mixtures reduces the flame temperature, which speeds up the CO oxidation reaction and slows down the CO_2 dissociation reaction. At the optimum equivalence ratio, the CO concentration reaches its minimum level. After this point, further decreasing the equivalence ratio causes the CO emissions

42

to increase. This is because the flame temperature and the CO oxidation reaction rate become too low, and the residence time required for the CO oxidation reaction to take place became longer than the residence time in the combustor, causing a rapid rise in CO concentration. At the critical LBO equivalence ratio, the flame reaches the lowest temperature and the highest CO concentration [11].

In this thesis, CO emission measurements were performed for lean blowout experiments to detect proximity to the lean blowout limit for various fuel mixtures. The CO measurements in the exhaust gas were carried out using a non-dispersive infrared (NDIR) gas analyzer (Horiba). The emission sampling probe was located 50 mm upstream of the combustion liner exit. The upper CO detection limit was 1000 ppm. Samples were collected for at least 120 seconds for each operation point. All emissions were measured dry (using a cold trap at 276 K) [58].

44

6. RESULTS AND SUMMARY OF THE PUBLICATIONS

This doctoral thesis is based on the results of 7 peer-reviewed papers and consists of two parts. The first and main part is focused on lean blowout and flashback of various fuel mixtures that can be of interest for gas turbine applications. This part of the work was mostly carried out by the author and led to 4 journal papers and one peer reviewed conference paper. These papers have built the main body of the thesis. The second part was focused on studying the autoignition of various fuel/air mixtures in a turbulent flow reactor. In this part, the candidate had a secondary role which mainly involved chemical kinetic modeling of the experimental results and participating in the experimental measurements. This part of the work resulted in three journal publications, two of which are included in the thesis.

The main part of this chapter is devoted to the results obtained from the lean blowout and flashback experiments. Thereafter, some of the autoignition results that are most relevant to the flashback and lean blowout studies are presented. Finally, a short summary of the above-mentioned papers followed by the contribution of the candidate in each paper is presented. A more detailed presentation of the results can be found in the papers appended to this thesis.

6.1. Lean blowout and flashback in the variable-swirl combustor

6.1.1. Test conditions and fuel mixtures

Swirl number

The swirl number of the flow entering the combustor was varied by changing the proportion of tangential to axial flow through the swirler. The swirl number was determined for various axial/tangential mass flow ratios, by measuring the axial and

45

tangential velocity profiles 1 mm above the dump plane of the combustor using LDA. The swirl number for each flow condition was calculated using Eq. (5). For lean blowout and flashback experiments, the swirl number was varied between 0.00 and 0.66. Figure 14 shows the calculated swirl number as a function of axial/tangential momentum ratio. Figure 15 demonstrates the axial velocity profiles at different swirl numbers. This figure indicates that by varying the swirl number between 0.06 and 0.66, the flow field changed drastically in the combustor.
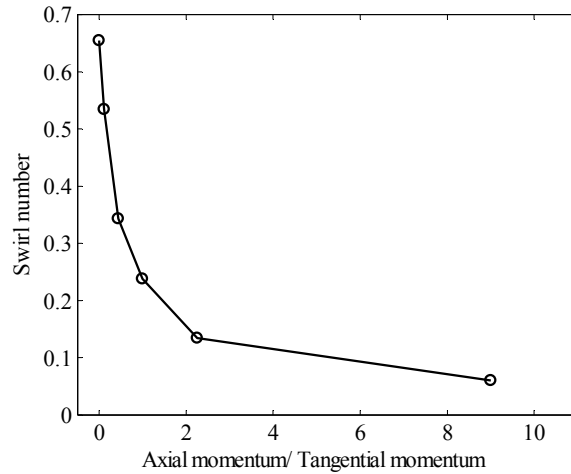
Figure 14.
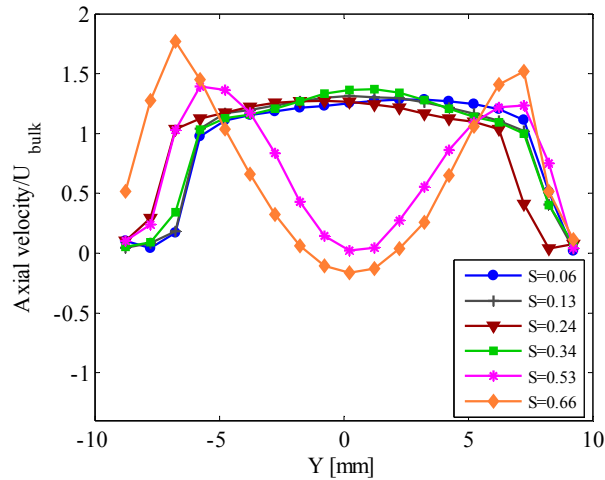Swirl number as a function of ratio of axial/tangential momentum.

Figure 15.
Normalized axial velocity profiles obtained from LDA measurements for different swirl numbers.

46

Fuel composition

Fuel mixtures used in the lean blowout and flashback experiments consisted of varying fractions of H_2, CO, CH_4, CO_2 and N_2. These mixtures were chosen to study the lean blowout and flashback of alternative fuels relevant for gas turbines such as syngas, biogas and hydrogen enriched natural gas.

Inlet temperature

The inlet air temperature was 650 K for the majority of the experiments. The effect of inlet temperature on lean blowout limit was investigated using three inlet temperatures of 450, 550 and 650 K (Paper **I**).

Air mass flow rate

The effect of total air mass flow rate on the lean blowout limit of CH_4 was studied using 7 different mass flow rates ranging from 100 to 475 SLPM (Paper **I**). The effect of total air mass flow rate on the flashback mechanism of CH_4/H_2 mixtures was studied by varying the mass flow rates between 75 and 200 SLPM. Table 2 demonstrates an overview of the fuel compositions and test conditions studied in the lean blowout and flashback experiments.

6.1.2. Lean blowout: effects of fuel composition and swirl number (Paper I and II)

The velocity measurements performed under non-reacting flow conditions indicated that varying the swirl number had a substantial impact on the flow field in the combustor. This observation created the motivation for performing further investigations regarding the effect of swirl number on the lean blowout of various fuel mixtures. Some of the obtained results are presented in this summary.

Generally, the lean blowout equivalence ratio of a given fuel mixture decreased with increasing swirl number within the studied range. This can be seen in Figure 16. where the lean blowout equivalence ratio is plotted as a function of swirl number for various fuel mixtures. Figure 16 shows that the effect of swirl number on the lean blowout limit varied depending on the fuel composition. As the H_2 fraction in the fuel mixture increased, the effect of the swirl number on the lean blowout equivalence ratio became less pronounced. Moreover, regardless of the swirl number, H_2 content of the fuel mixture seemed to have a significant influence on the equivalence ratio at which lean blowout occurred.

The visual observations of the flame indicated that swirl number played a substantial role on the structure and the dynamic behavior of the flame. Through the process of reducing the equivalence ratio from a stable flame to lean blowout, three distinct regimes were visually detected depending on the swirl number. Figure 17 shows broadband luminosity photographs of a flame in the low swirl number regime when decreasing the equivalence ratio.

47

Table 2.
Chemical composition of the fuel mixtures used for the experiments

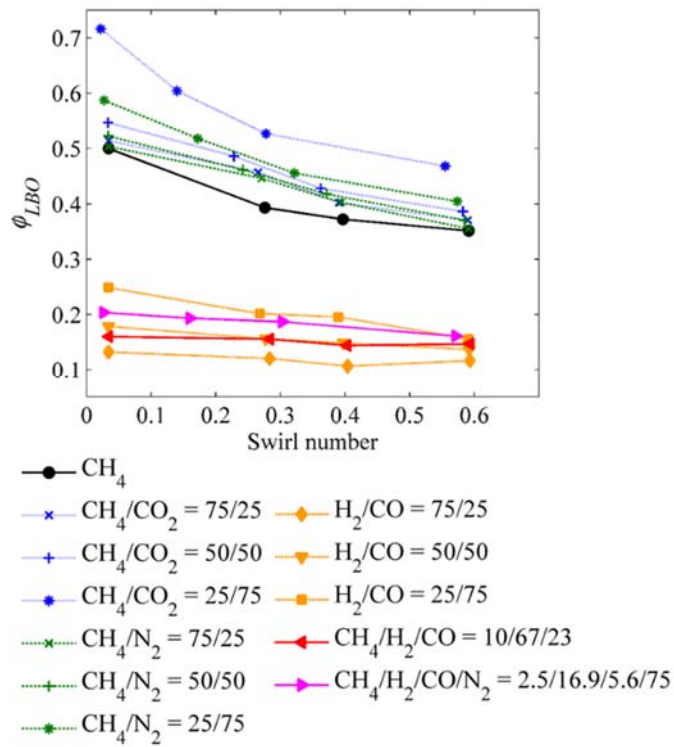| H$_2$	CO	CH$_4$	CO$_2$	N$_2$	Swirl number	Total air mass flow	Air preheat temperature	Type of study	Exp. setup	Published in
% molar composition						SLPM	K			
0.0	0.0	100.0	0.0	0.0		100-475	450-650			
0.0	0.0	75.0	25.0	0.0						
0.0	0.0	50.0	50.0	0.0	0.03, 0.29, 0.40, 0.60				Version I	
0.0	0.0	25.0	75.0	0.0		250	650	LBO		Paper I
0.0	0.0	75.0	0.0	25.0						
0.0	0.0	50.0	0.0	50.0						
0.0	0.0	25.0	0.0	75.0						
0.0	0.0	100.0	0.0	0.0						
25.0	75.0	0.0	0.0	0.0	0.03, 0.31, 0.42, 0.60				Version I	
50.0	50.0	0.0	0.0	0.0		250	650	LBO		Paper II
75.0	25.0	0.0	0.0	0.0						
67.5	22.5	10.0	0.0	0.0						
16.9	5.6	2.5	0.0	75.0						
10.0	0.0	90.0	0.0	0.0						
15.0	0.0	85.0	0.0	0.0	0.00, 0.24, 0.53, 0.66				Version II	
25.0	0.0	75.0	0.0	0.0		75-200	650	FB		Paper III
50.0	0.0	50.0	0.0	0.0						
75.0	0.0	25.0	0.0	0.0						
90.0	0.0	10.0	0.0	0.0						
10.0	0.0	90.0	0.0	0.0						
25.0	0.0	75.0	0.0	0.0						
50.0	0.0	50.0	0.0	0.0						
75.0	0.0	25.0	0.0	0.0						
90.0	0.0	10.0	0.0	0.0	0.66					
25.0	37.5	37.5	0.0	0.0						
40.0	40.0	20.0	0.0	0.0						
50.0	25.0	25.0	0.0	0.0		200	650	FB-LBO	Version II	Paper IV
60.0	20.0	20.0	0.0	0.0						
67.0	23.0	10.0	0.0	0.0						
75.0	12.5	12.5	0.0	0.0						
10.0	90.0	0.0	0.0	0.0						
25.0	75.0	0.0	0.0	0.0	0.53, 0.66					
50.0	50.0	0.0	0.0	0.0						
75.0	25.0	0.0	0.0	0.0						
90.0	10.0	0.0	0.0	0.0						

48

Figure 16.
Lean blowout equivalence ratio of various fuel mixtures as a function of swirl number.
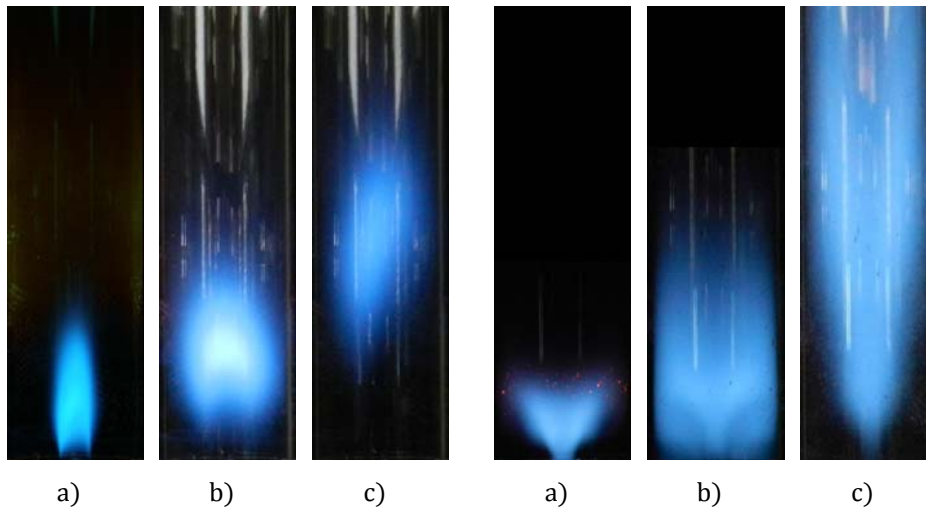

| a) | b) | c) |

Figure 17.
Broadband luminosity photographs of a H_2/CO flame at $S = 0.03$ (low swirl case) and a) $\phi = 0.50$, b) $\phi = 0.25$, c) $\phi = 0.21$.

| a) | b) | c) |

Figure 18.
Broadband luminosity photographs of a H_2/CO flame at $S = 0.59$ (high swirl case) and a) $\phi = 0.25$, b) $\phi = 0.19$, c) $\phi = 0.15$.

49

In the low swirl number regime, reducing the equivalence ratio was associated with high amplitude oscillations of the flame position between an attached and a lifted flame. The amplitude of the oscillations became increasingly larger until blowout occurred.

In the high swirl number regime the lean blowout process was a smooth transition between an attached stable heart-shaped flame to a lifted narrow tornado-shaped flame which blew out of the combustor smoothly. Figure 18 shows broadband luminosity photographs of a flame in the high swirl number regime when decreasing the equivalence ratio.

In the moderate swirl number regime, the flame underwent one and sometimes two consecutive phases when reducing the equivalence ratio. In the first phase, the flame behaved the same way as it did in the low swirl number regime. The interesting observation was that sometimes the flame survived the high-amplitude oscillations and reached a stable lifted position, which was similar to the high swirl number regime. This means that in the moderate swirl number regime two different but repeatable lean blowout equivalence ratios were obtained. Figure 19 presents an overview of the lean blowout process indicated for these swirl numbers.
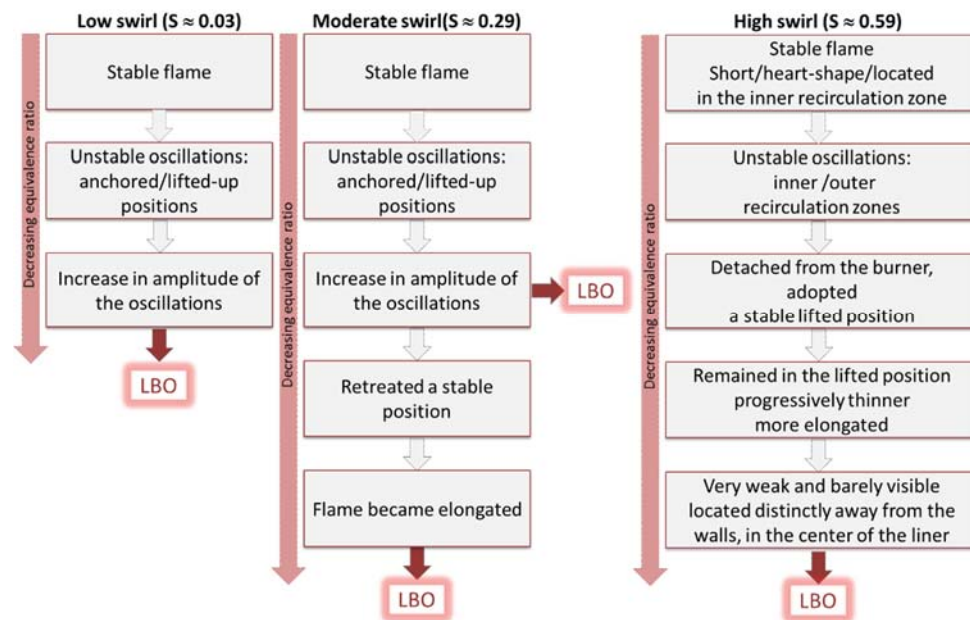

Figure 19.
An overview of the lean blowout process that was visually indicated for low, moderate and high swirl numbers.

50

6.1.3. Flashback mechanisms (Paper III)

As discussed in section 2.3.2, flashback occurs when the flame leaves its stable position in the combustor and starts propagating against the incoming unburned fuel/air mixture into the premixing section. From a more fundamental point of view, as a turbulent propagating flame, flashback is a result of the interaction between the flow field, chemical kinetics and transport properties of the reactants. Given the high reactivity of hydrogen containing fuels, flashback poses a great risk when using such fuels in premixed gas turbine combustors

Having this in mind, the first flashback study conducted in this thesis was focused on investigating the mechanisms that can initiate flashback for CH_4/H_2 mixtures in the variable-swirl combustor. The flow field in the combustor was altered by varying the swirl number and air mass flow rate. The chemical kinetics and transport properties of the reactants were varied by changing the H_2 molar fraction, These operating conditions are presented in Table 2 together with the fuel composition used in the experiments. For a given air mass flow rate, swirl number and H_2 molar fraction, flashback was triggered by gradually increasing the equivalence ratio. OH^*-chemiluminescence imaging was used to visualize the onset of flashback and propagation of the flame in the premixing section. The highlights of the findings of this study are presented in the following paragraphs. More detailed description of the work can be found in Paper **III**.

By varying the swirl number, air mass flow rate and H_2 fraction of the fuel mixture, three different flashback mechanisms were observed. These mechanisms were:

1- Flashback caused by combustion induced vortex breakdown (CIVB)
2- Flashback in the boundary layer (BL flashback)
3- Flashback caused by autoignition.

Figure 20 demonstrates a map of the flashback mechanisms and the test conditions under which they were observed. In this figure the green areas refer to the flashback-free operating conditions and the white areas represent the conditions that were not tested in this study.

Flashback caused by CIVB

Figure 20 indicates that CIVB flashback occurred for any given H_2 mole fraction at swirl numbers > 0.53. The existence of a recirculation zone at these swirl numbers was confirmed by the LDA velocity measurements conducted at the inlet of the combustor. The OH^*-chemiluminescence images of flashback under these conditions showed that by increasing the equivalence ratio flashback was initiated in the center of the combustor inlet. The flame front propagated as a narrow filament along the central axis of the premixing section. This can be seen in Figure 21, where OH*-chemiluminescence images of a CIVB flashback event which occurred at swirl number of 0.66 and H_2 mole fraction of 0.9 are shown.

It is important to note that this type of flashback did not occur as a continuous upstream flame propagation. This means that before permanently stabilizing in the premixing section, the flame traveled back and forth between the premixing section and the combustor. This observation was later studied more thoroughly in a separate measurement campaign, the results of which were published in Paper **V**.
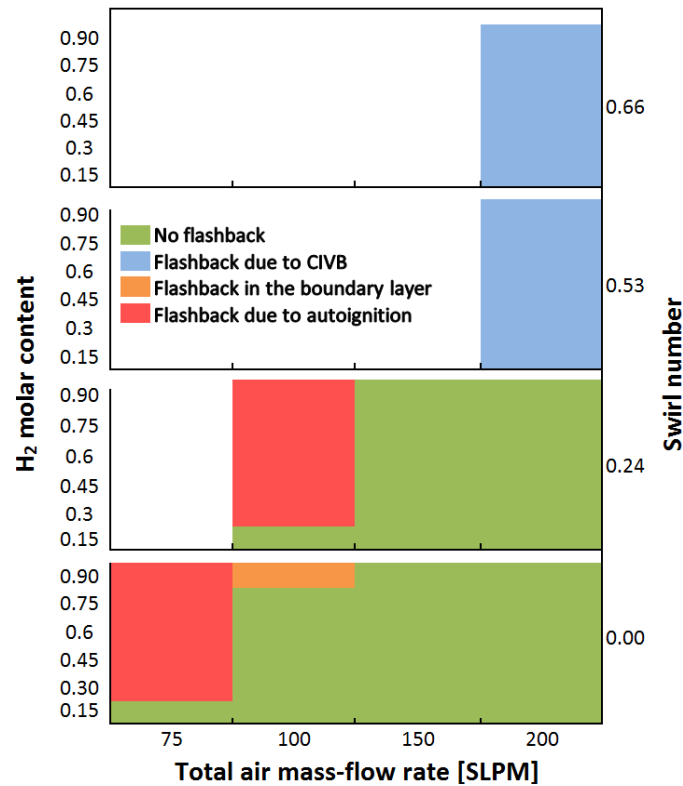

Figure 20.
Different flashback mechanisms observed under various test conditions.

Flashback in the boundary layer

As it can be seen in Figure 20, flashback in the boundary layer occurred at an air mass flow rate of 100 SLPM and at swirl number of 0.00. The OH[*]-chemiluminescence images of the flashback event under this condition (Figure 22), indicate that the flashback was initiated at the walls of the premixing section. When the flame propagated in the premixing section it was inclined with its tip towards the walls of the tube. Once flashback started in the boundary layer, the flame propagated only in the upstream direction throughout the entire flashback event which was in contrast to the CIVB flashback, where it could advance and recede several times.
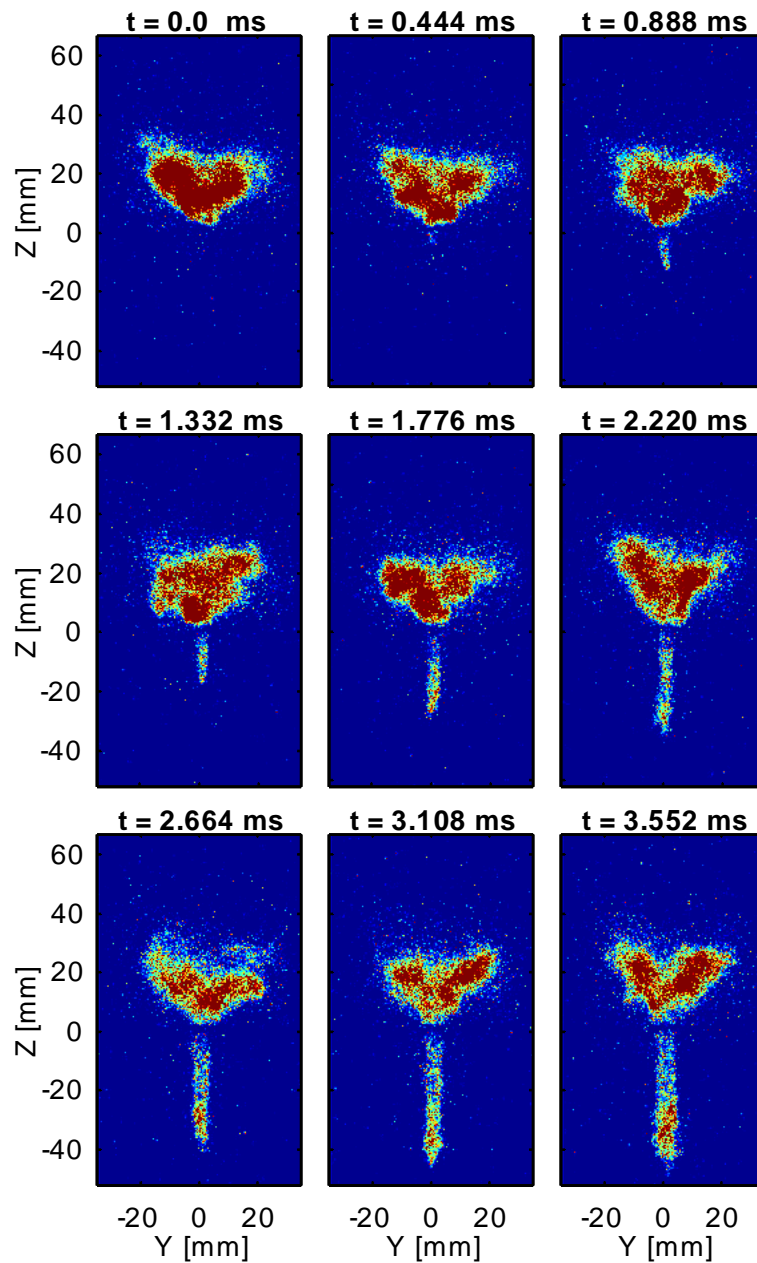
52

Figure 21.
OH*-chemiluminescence image sequence of upstream flame propagation caused by CIVB.
Image interval = 0.444ms, exposure time= 72μs, swirl number = 0.66, fuel H_2 mole fraction = 0.9,
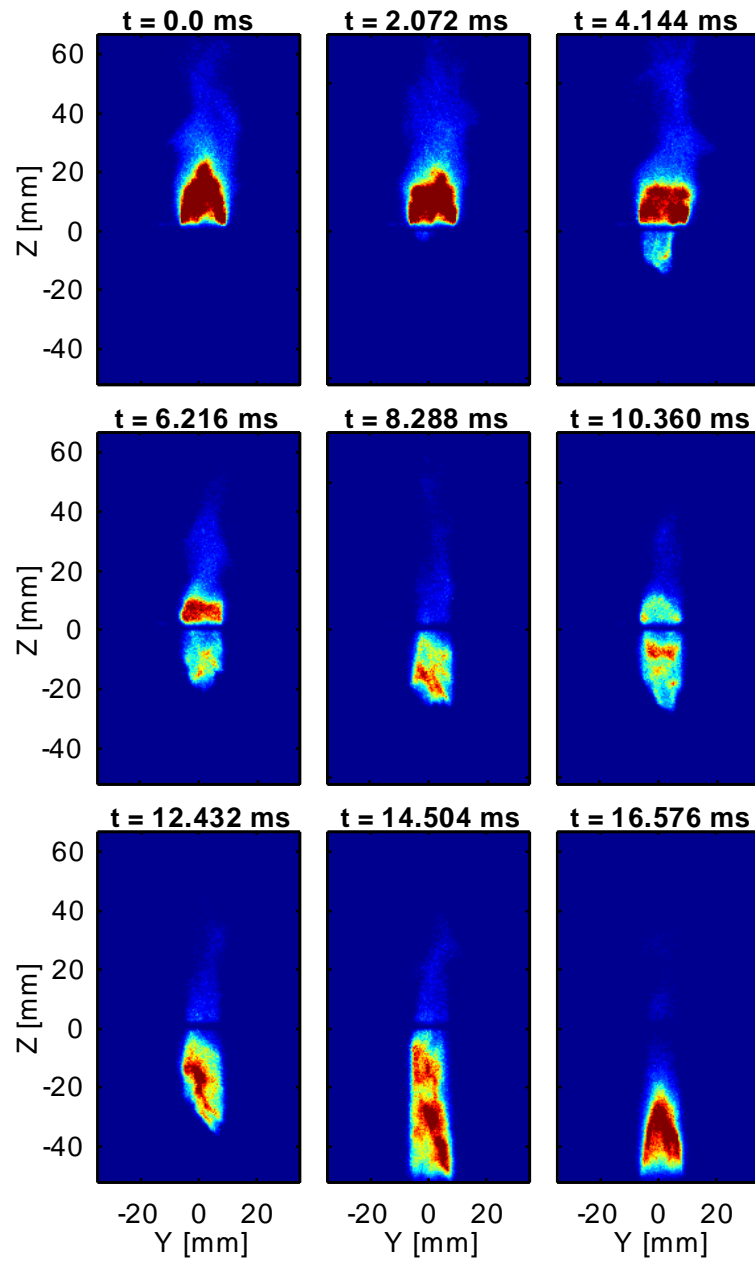$\Phi = \Phi_{FB} = 0.234$.

Figure 22.
OH*-chemiluminescence image sequence of upstream flame propagation in the boundary layer.
Image interval = 2.072 ms, exposure time = 72 μs, swirl number = 0.0, fuel H_2 mole fraction = 0.9,
$\phi = \phi_{FB} = 0.671$.

54

Flashback caused by autoignition

As indicated in Figure 20, this type of flashback was observed at low mass flow rates (100 and 75 SLPM) and low swirl numbers (S = 0.00 and 0.24). Under these conditions, while a lifted flame existed in the combustor, a second flame was formed upstream of the optical section of the premixing section. This secondary flame then propagated through the premixing section. It entered the combustor, joined the existing flame and caused flame blowout in the combustor. This event was extremely fast. It was therefore impossible to have any visual memory of the event with naked eyes. However, the load noise of the autoignition event allowed for saving a recording of the event in the memory of a running high-speed camera. OH^*-chemiluminescence image sequences of this type of event are shown in Figure 23 and Figure 24. Estimating the bulk residence time in the premixer, in combination with gas-phase chemical kinetic modeling (Chemkin), suggested that the residence time of the reactants in the premixer (0.01 s) was significantly shorter than the ignition delay calculated from chemical kinetic modeling under these conditions (> 1.5 s). This would suggest that autoignition should be precluded under these conditions. However, it has been reported that recirculation zones can significantly increase the effective residence time of the reactants and thereby assist autoignition [37]. Further to this, autoignition experiments conducted in the turbulent flow reactor (Paper **VI**) showed that surface reactions on the walls of premixing sections significantly reduced ignition delays below what is predicted by gas-phase kinetic modeling. This suggests that this type of flashback can be more important for combustor premixing section designs with more reactive surfaces and with a high surface/volume ratio.

Flashback speed

In order to quantify the differences in flashback speed between the three flashback mechanisms, the temporal and spatial propagation of the flame was studied using OH^*-chemiluminescence images. To estimate the flame front boundaries, the images were thresholded based on the gradient of the pixel counts in the images. Thereafter, the incremental flame front displacement between each two consecutive frames was estimated for several flashback events of each mechanism. By using a linear approximation to the flame front displacement, the flashback speed was estimated for different mechanisms. Figure 25 demonstrates the flame front displacement in the premixing section as a function of time for the CIVB and BL flashback events together with the linear approximations. This figure indicates that the speed at which the flame propagated through the premixing section was significantly higher for the CIVB flashback than for the BL flashback.
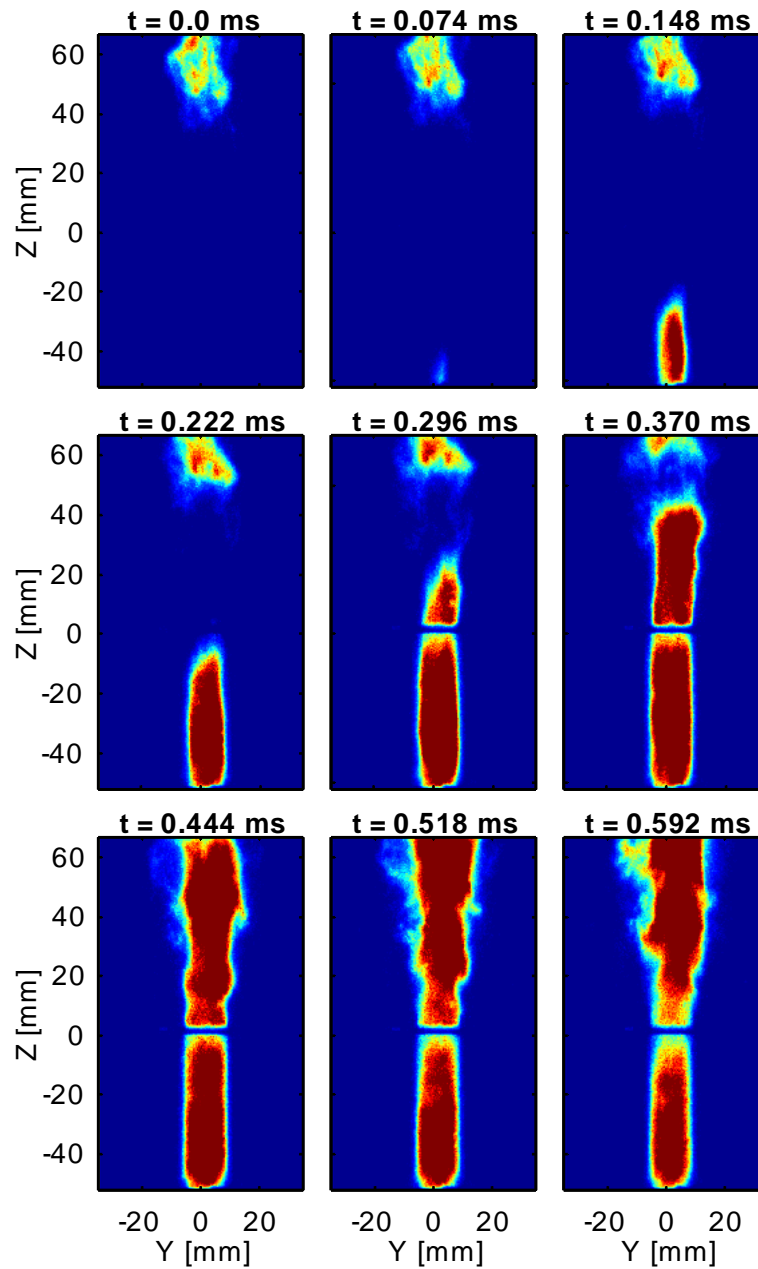
55

Figure 23
OH*-chemiluminescence image sequence of upstream flame propagation caused by autoignition.
Image interval = 0.074 ms, exposure time = 72 μs, swirl number = 0.24, fuel H$_2$ mole fraction = 0.15,
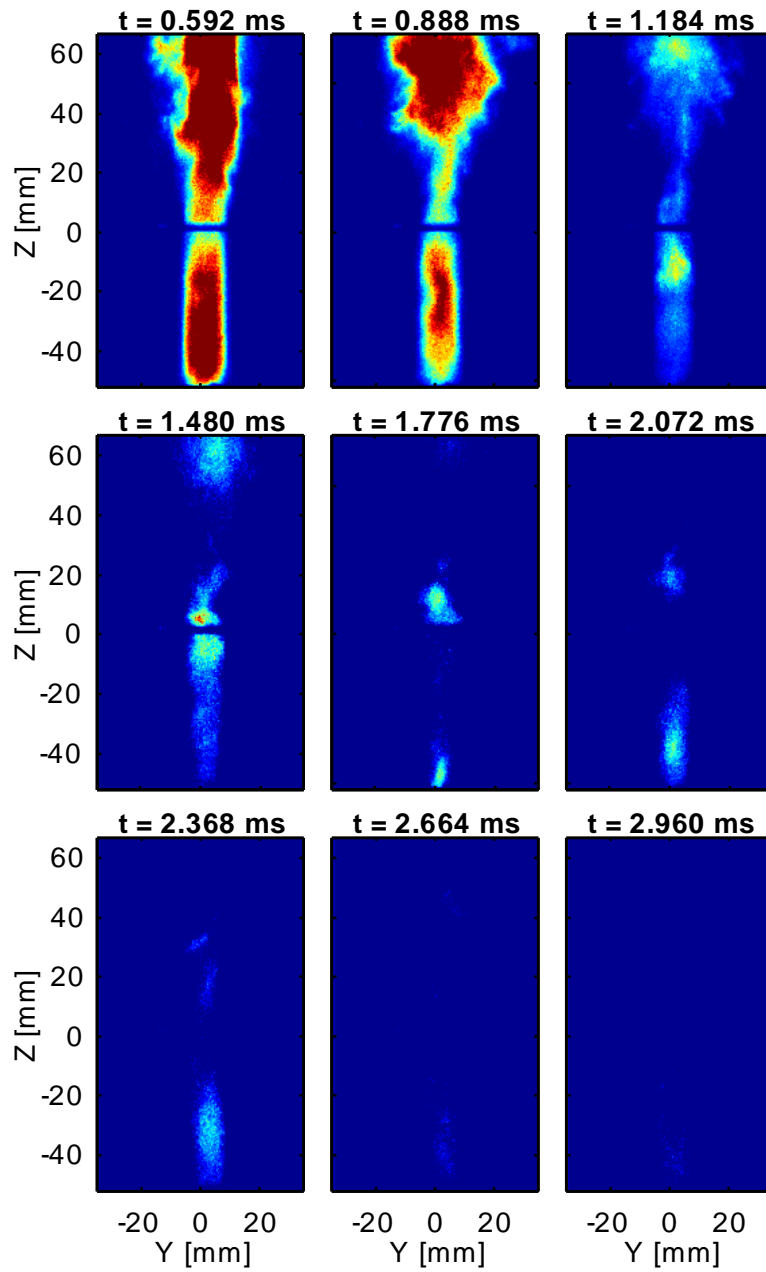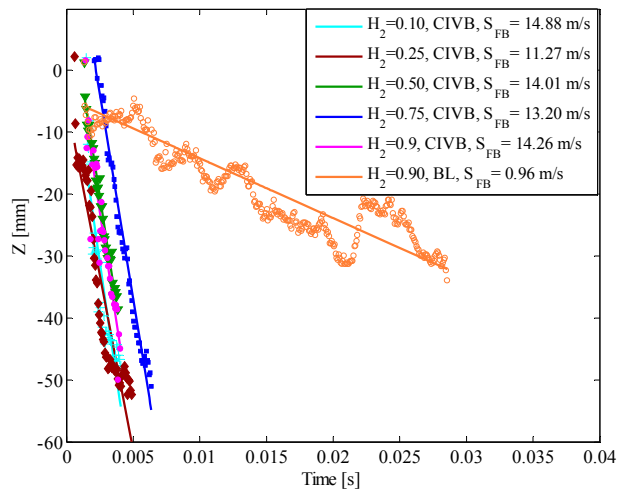$\phi = \phi_{FB} = 0.696$.

Figure 24.
OH*-chemiluminescence image sequence of blowout of the flame due to autoignition.
Image interval = 0.074 ms, exposure time = 72μs, swirl number = 0.24, fuel H_2 mole fraction = 0.15,
$\phi = \phi_{FB} = 0.696$.

Figure 25.
Linear approximation of the flame front displacement for various fuel H_2 mole fraction /flashback mechanisms.

As noted before, in the case where flashback occurred due to autoignition, a second flame propagated in the direction of the unburned gases. For this reason, the flashback speed for this case is considered the speed at which the second flame propagated through the premixing section towards the combustor. The displacement of the second flame front during the flashback event is shown in Figure 26. The data presented in this graph was extracted from four independent flashback events recorded under the same experimental condition, and was highly repeatable. A linear fit to the flame front displacement yielded a flashback speed of 346 m/s.

6.1.4. Stability limits (Paper IV)

The results of the previous experiments conducted in the variable-swirl combustor showed that swirl number had a significantly larger effect on the flashback limit than it had on the lean blowout limit of a given fuel mixture. This suggested that altering the swirl number may be a plausible way for widening the stability range of the combustor when using syngas fuels. Paper **IV** was thus focused on investigating this idea. The lean blowout and flashback limits of 17 various syngas mixture (see Table 2) were investigated. In order to have a swirl stabilized combustion, the swirl numbers used in this study were to be sufficiently high to ensure the formation of a recirculation zone in the combustor. Two swirl numbers of 0.53 and 0.66 were used in this study, whose velocity profiles were measured previously at the inlet of the combustor (see Figure 15). The detailed description of the work and the results can be found in Paper **IV**.
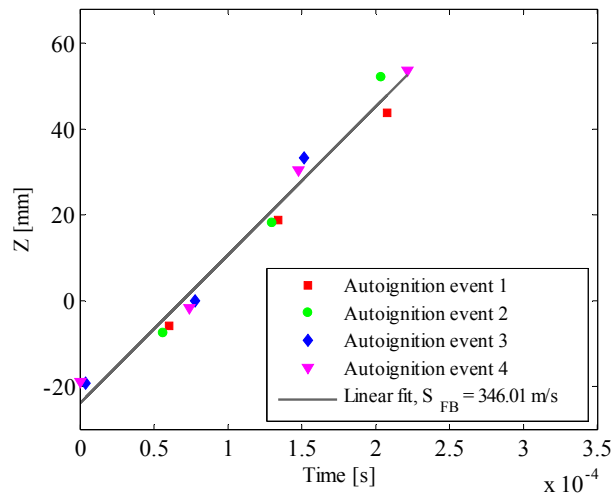
58

Figure 26.

The displacement of the second flame front in the premixing section obtained in four flashback events caused by autoignition under the same condition:
swirl number = 0.24, fuel H_2 mole fraction = 0.15, $\phi = \phi_{FB}$ = 0.696.

Effect of swirl number on the stability range

Figure 27 demonstrates the lean blowout and flashback equivalence ratios for binary mixtures of H_2/CO at two swirl numbers of 0.53 and 0.66. This figure indicates that, for all of the tested fuel mixtures, the stability range was greatly enhanced when reducing the swirl number from 0.66 to 0.53. The effect was more pronounced for mixtures with a lower H_2 content. On one hand, the presence of a recirculation zone in the combustor may imply that flashback was caused by combustion induced vortex breakdown at both swirl numbers. On the other hand, the significantly different flashback limits of the tested fuels at $S = 0.66$ and $S = 0.53$, suggested that flashback may have been triggered by different mechanisms at $S = 0.66$ and $S = 0.53$. This called for further velocity measurements and visual investigations of the flame flashback. To identify the differences between the flow fields at these swirl numbers, PIV measurements were performed for non-reacting as well as for combusting cases at various equivalence ratios. The velocity measurements revealed substantial differences between $S = 0.66$ and $S = 0.53$ in how the flow field evolved when the equivalence ratio was increased as flashback was approached.
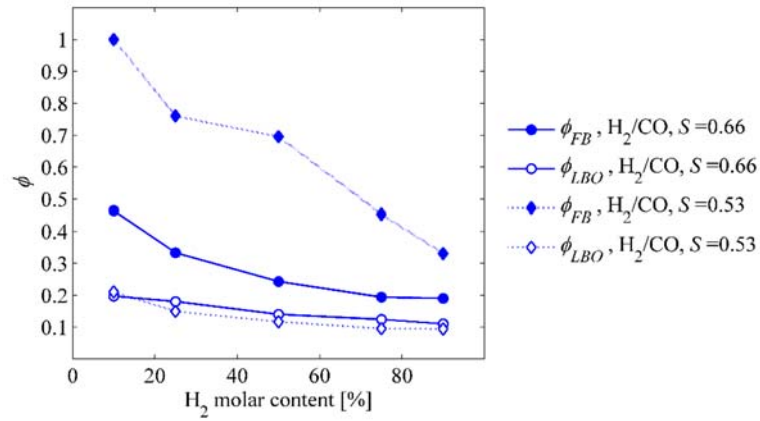
59

Figure 27.
FB and LBO equivalence ratio as a function of H_2 molar content of the fuel mixture for $S = 0.66$ and $S = 0.53$ for binary mixtures of CO/H_2.

Velocity field in the combustor at swirl numbers of S = 0.66 and S = 0.53

Figure 28 shows the axial velocity field in the combustor obtained for the non-reacting flow for $S = 0.66$. Figure 29 shows reacting flow at $\phi = 0.387$ where a stable flame was present in the combustor and Figure 30 shows reacting flow at $\phi = \phi_{FB}$ prior to flashback for $S = 0.66$. At $S = 0.66$ the flow field featured an inner recirculation zone, an annular high-velocity zone and an outer recirculation zone between the high-velocity zone and the bounding walls. These figures indicate that the main characteristics of the flow field remained unchanged as the equivalence ratio was increased from $\phi = 0.0$ (non-reacting flow) to the flashback equivalence ratio.
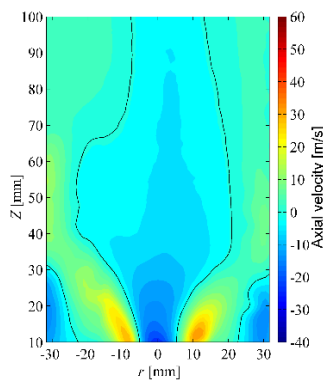

Figure 28.
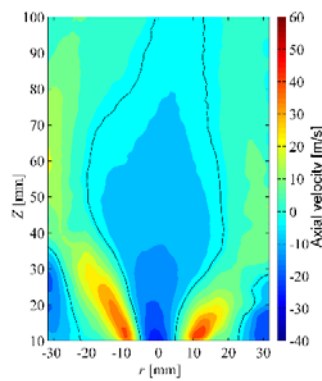Axial velocity field in the combustor for S = 0.66 & $\phi = 0.0$ (non-reacting flow).

Figure 29.
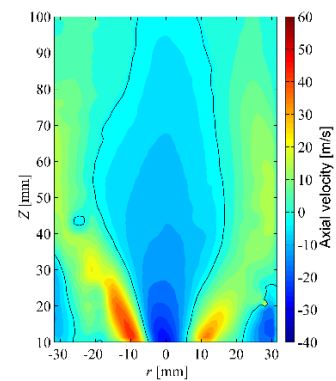Axial velocity field in the combustor for S = 0.66 & $\phi = 0.387$, for a H_2/CH_4 mixture (50:50).

Figure 30.
Axial velocity field in the combustor for $S = 0.66$ & $\phi = 0.429$, for a H_2/CH_4 mixture (50:50).

60

Figure 31 to Figure 34 show the axial velocity field in the combustor obtained at different equivalence ratios for $S = 0.53$. Figure 31 corresponds to the non-reacting flow, while Figure 32 and Figure 33 correspond to different equivalence ratios at which a stable flame was sustained in the combustor. Figure 34 shows the axial velocity field at $\phi = \phi_{FB}$ prior to flashback. These figures indicate that the recirculation zone that existed in the combustor in the non-reacting case and at low equivalence ratios vanished from the combustor as the equivalence ratio was increased.
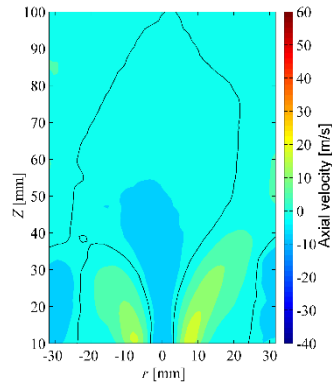

Figure 31.
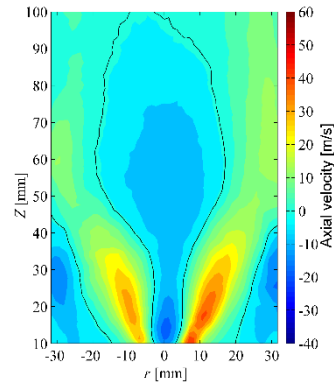Axial velocity field in the combustor for $S = 0.53$ & $\phi = 0.0$ (non-reacting flow).

Figure 32.
Axial velocity field in the combustor for $S = 0.53$ & $\phi = 0.447$, for a H_2/CH_4 mixture (50:50).
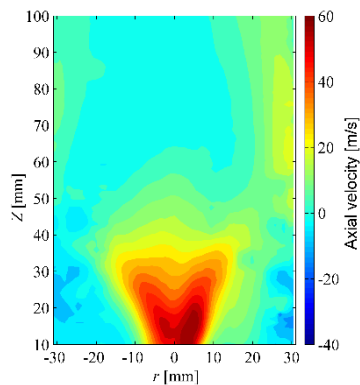
Figure 33.
Axial velocity field in the combustor for $S = 0.53$ & $\phi = 0.595$, for a H_2/CH_4 mixture (50:50).
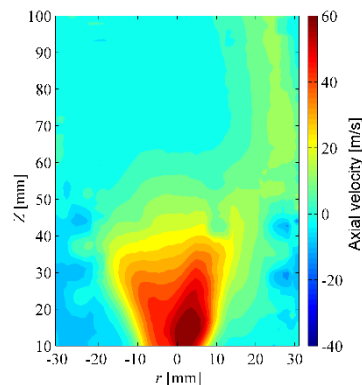
Figure 34.
Axial velocity field in the combustor for $S = 0.53$ & $\phi = 0.714$, for a H_2/CH_4 mixture (50:50).

It should be noted that this change in the flow field occurred at equivalence ratios that were far below the flashback limit. This means that even though no recirculation zone was present in the flow field, a stable flame was sustained in the

61

combustor. By further increasing the equivalence ratio, the main features of the flow field remained unchanged until flashback occurred. With no recirculation zone in the flow field, the CIVB was ruled out as being the triggering mechanism for flashback at $S = 0.53$.

OH^*-chemiluminescence images of the flame during flashback at S = 0.66 and S = 0.53

In order to obtain more information regarding the mechanism that caused flashback at $S = 0.53$, OH^*-chemiluminescence images of the flame were recorded prior to and during flame flashback for this swirl number. These images were then compared to those recorded for $S = 0.66$. This was to identify the underlying differences between how flashback was initiated and proceeded at these swirl numbers. Figure 35 and Figure 36 demonstrate sequences of OH^*-chemiluminescence images recorded during a flashback event for $S = 0.66$ and $S = 0.53$, respectively.

The main differences indicated by comparing Figure 35 with Figure 36 have been summarized in the list below. A more detailed discussion of these results can be found in Paper **IV.**

Before flashback, at $S = 0.53$, the flame was stabilized in the shear layer with two distinct anchoring points whereas at $S = 0.66$, the flame was stabilized in the combustor through a single anchoring point.

At the onset of flashback, at $S = 0.53$, the flame was drawn upstream towards the two anchoring points before propagating into the premixing section with a sharp conical front whereas at $S = 0.66$, flashback started as a narrow filament that was propagating in the centerline of the premixing section. The propagating flame front at $S = 0.53$ had a significantly broader radial width than that of the higher swirl number $S = 0.66$.

After the flame propagated the entire length of the premixing section, at $S = 0.53$, the flame was stabilized at the bottom of the premixing section, whereas at $S = 0.66$, the flame was still extended into the combustor.

Considering these visual observations of flashback in the premixing section together with the axial velocity field in the combustor, it was concluded that at $S = 0.53$, flashback was initiated by competition between the flame speed and the flow velocity in the core flow. It is noted that although at $S = 0.53$, the flashback did not start in the boundary layer, as the flame propagated further upstream in the premixing section, it extended radially to the walls. At this point, both mechanisms, flashback in the core flow and flashback in the boundary layer, contributed to the further upstream propagation of the flame.

62

Figure 35.
OH*-chemiluminescence of the flame at flashback for $S = 0.66$ for a H$_2$/CH$_4$ mixture (50:50). The white lines show the boundaries of the premixing section and the inlet of the combustor.
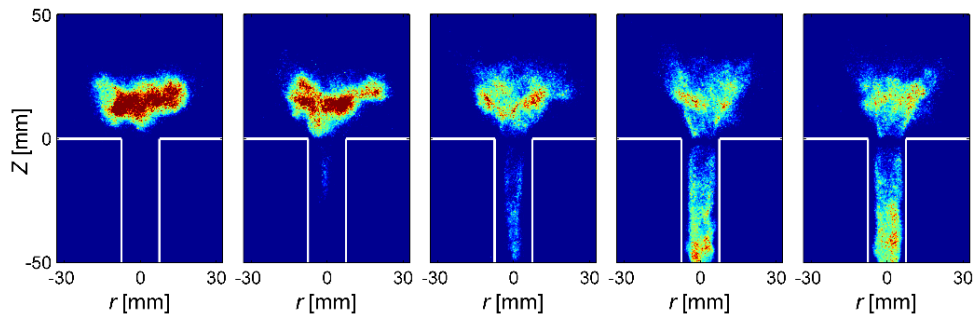

Figure 36.
OH*-chemiluminescence of the flame at flashback for $S = 0.53$ for a H$_2$/CH$_4$ mixture (50:50). The white lines show the boundaries of the premixing section and the inlet of the combustor.
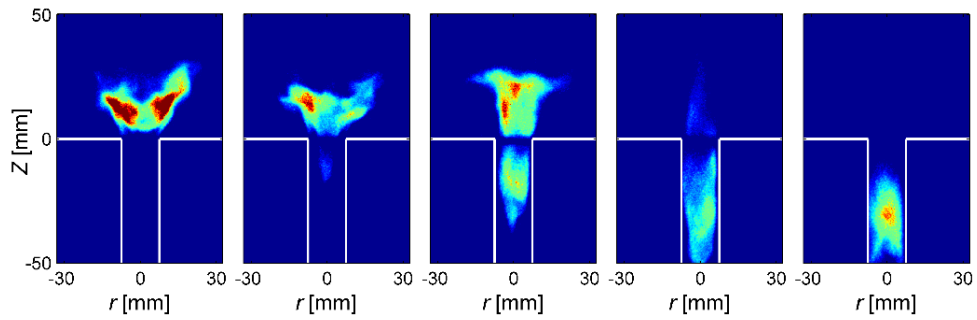
6.2. Autoignition in the turbulent flow reactor

As an important operability risk, autoignition must be avoided in lean premixed combustors. Similar to flashback, autoignition poses a risk when using hydrogen containing fuels in lean premixed gas turbine combustors. The flashback experiments performed in the variable-swirl combustor showed that the occurrence of autoignition can result in flame propagation in the premixing section, blowout and severe disruption of the combustors operation. The experimental setup was designed and built at the division of thermal power engineering by Dr. Alessandro Schönborn. The results that will be presented hereafter, are selected from the study that was performed on the autoignition of hydrogen (Paper **VII**).

6.2.1. Visualization of autoignition

As noted previously, occurrence of autoignition in the premixer of a gas turbine combustor can cause severe damage. The consequences of autoignition may become even more catastrophic when the autoignition event is followed by flame flashback. To investigate this phenomenon, autoignition of H_2/air mixtures was visualized in the turbulent flow reactor using high-speed OH^*-chemiluminescence imaging. During the experiments, the conditions in the flow reactor were set such that the autoignition occurred in the optical test section of the reactor and could thus be recorded with a high-speed camera. The detailed discription of the experimental method can be found in Paper **VII**. Figure 37 demonstrates OH^*-chemiluminescence sequence of an autoignition event for a H_2/air mixture. The process of autoignition followed by deflagration and eventually flame flashback can be seen in this figure: The autoignition kernels appear in several locations along the central axis of the reactor; the kernels then expand and merge with each other through deflagration at which point flashback occurs in the flow reactor.
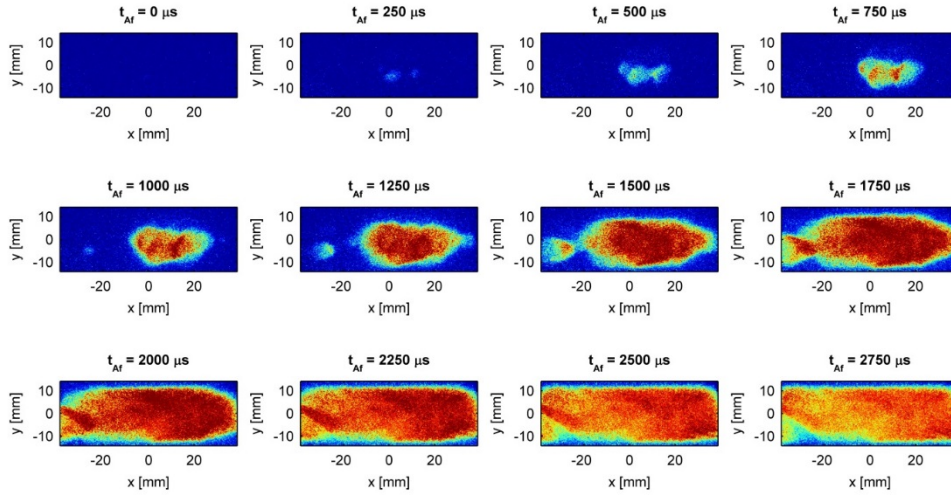
Figure 37.
OH*-chemiluminescence sequence of hydrogen autoignition in air at $T = 850$ K, $p = 0.8$ MPa, $\phi = 0.25$, $\tau = 211$ ms, and $Ui = 13.8$ m/s, showing the nucleation of multiple kernels followed by deflagration and flashback.

Turbulent flame speed in the reactor

Temporal and spatial evolution of the autoignition kernels can be quantified by means of few simplifications. First, the boundaries of the kernels can be estimated by thresholding the images based on the gradient of pixel counts in the images. Next, the expansion of a kernel in time can be calculated by assuming spherical dimensions for the kernels and knowing the time interval between the images. Finally, by knowing the density of the burned and unburned gases the turbulent flame speed can be estimated based on Eq. (23):

$$S_T = u_r \left(\frac{\rho_b}{\rho_u} \right) \tag{23}$$

where S_T is the turbulent flame speed through the unburned mixture, u_r is the propagation velocity of the flame kernel radius, ρ_u is the density of the reactants and ρ_b is the density of the burned gases.

By using the above-mentioned procedure, an average turbulent flame speed of 7.4 m/s was obtained for a flashback event presented in Figure 37. For this case, the initial velocity of the unburned gases was 13.8 m/s, which was well above the estimated flame speed. This may be explained considering how the velocity of the incoming flow is affected by a transient autoignition event: When autoignition occurs in the middle of the test section, the kernel expands in both upstream and downstream directions consuming the unburned reactants. Assuming a constant pressure in the reactor, the velocity of the outgoing flow remains unaffected during autoignition. This is because the discharge valve still operates on unburned gases

with the same density. This means that, the incoming flow slows down due to occurrence of autoignition, which explains why the autoignition flame can flashback even when the initial inlet velocities are far above the turbulent flame speed.

In this respect, the turbulent flame speed obtained from Eq. (23) may be used to identify the critical flow velocity at which flame stabilization occurs after an autoignition event. Figure 38 shows a schematic of an autoignition event in a plug-flow reactor at t_0 and after a time step of Δt.
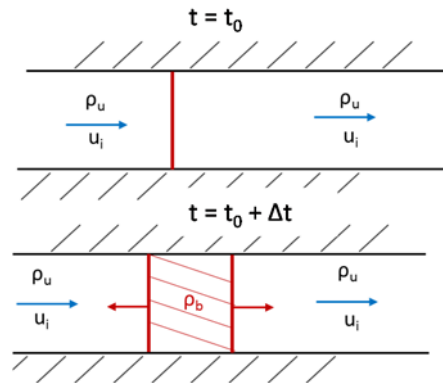

Figure 38.
Flame front stabilization of autoignition kernel in plug-flow.

As illustrated by the hatched area, the expansion of the gases after a time step of Δt, due to upstream and downstream kernel expansion for a constant cross section area of the reactor (A) can be calculated as:

$$\Delta V = 2S_T \left(\frac{\rho_u}{\rho_b} - 1 \right) A \tag{24}$$

Assuming that the outgoing flow velocity remains the same as the initial incoming velocity prior to autoignition, U_i, the 'updated' final incoming flow velocity after autoignition, U_f, will be:

$$U_f = U_i - 2S_T \left(\frac{\rho_u}{\rho_b} - 1 \right) \tag{25}$$

Stabilization of the autoignition flame may occur if the updated final incoming flow velocity matches the turbulent flame speed:

$$U_f = S_T \tag{26}$$

Using Eq. (25) and (26), the initial incoming velocity required for flame stabilization can thus be calculated:

$$U_i = S_T \left(2\frac{\rho_u}{\rho_b} - 1 \right) \tag{27}$$

Further experiments indicated temporary flame stabilization at an equivalence ratio of $\phi = 0.25$, a pressure of $p = 1.0$ MPa and a temperature of $T = 850$ K and $U_i = 12.88$ m/s. Visualization of such a flame using OH*-chemiluminescence is shown in Figure 39.
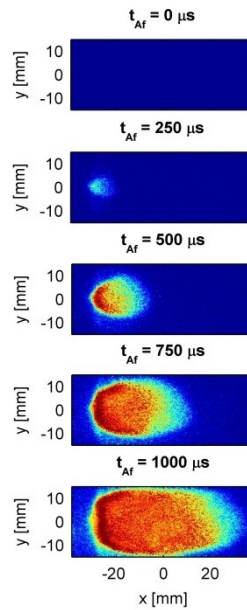

Figure 39.
OH*-chemiluminescence sequence of hydrogen autoignition in air at $T = 850$ K, $p = 1.0$ MPa, $\phi = 0.25$, $U_i = 12.88$ m/s, $U_f = 5.18$ m/s, showing temporary kernel stabilisation when $U_f = S_T$.

6.2.2. Ignition delays of a H₂/air mixture in the flow reactor

Flow reactors are suitable experimental apparatus for autoignition studies with relevance to gas turbine premixers because they operate at long ignition delays, low temperatures, constant pressures, and rely on turbulent mixing. Along with the visualization of H_2/air autoignition, the ignition delays of a H_2/air mixture were measured in the flow reactor at varying temperatures and pressures. Comparing the experimental results to the predictions of a plug-flow reactor model using homogenous gas-phase reactions showed that:
- The measured ignition delays were shorter than the predictions of the chemical kinetic model.
- The activation energy estimated using the experimental results was significantly lower than the activation energy obtained from the chemical kinetic model.

67

- The experiments indicated that increasing the pressure while maintaining the autoignition temperature resulted in shorter ignition delays. This trend was in contrast with the predictions of the chemical kinetic model.

The shorter ignition delays and lower activation energies indicated an accelerated autoignition process in the experiments in comparison with the chemical kinetic calculations. This may have been caused by the surface reactions taking place on the walls of the reactor. In addition, by increasing the pressure while maintaining the temperature and the surface area of the reactor, the surface area with respect to the amount of the reactants increased. This may also suggest that increasing the pressure leads to higher catalytic reactivity and thus shorter ignition delays for a given H_2/air mixture. To test this hypothesis, the gas phase reactions were combined with surface reactions occurring on the austenitic stainless steel walls of the reactor. This was done by adapting the surface reaction model of Deutschmann [72], which was originally developed for platinum, to the current study. A detailed description of the method can be found in Paper **VII**. The chemical kinetic calculations were repeated using the new mechanism. Figure 40 demonstrates the experimental results together with the chemical kinetic model predictions. As it can be seen, including surface reactions in the mechanism improved the model predictions in terms of the values of the ignition delays, the relationship between the ignition delays and pressure, and finally the magnitude of the slope of the ignition data.
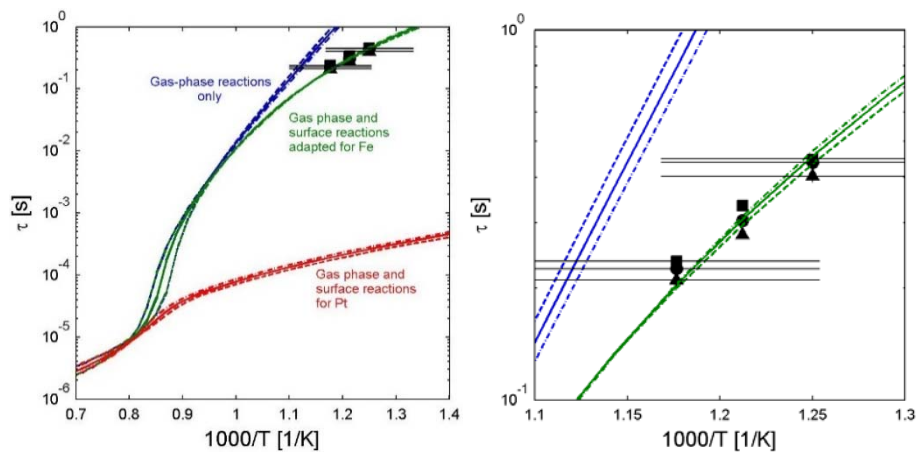

Figure 40.
Experimentally determined ignition delays and chemical kinetic modelling using a combination of surface and gas phase reactions. Symbols experiment, lines modelling ▲ 0.8 MPa ● 1.0 MPa ■ 1.2 MPa - - 0.8 MPa — 1.0 MPa – · – 1.2 MPa.

68

6.3. Summary of the publications

I. **Parisa Sayad**, Alessandro Schönborn, Denny Clerini, Jens Klingmann, ''Experimental investigation of methane lean blowout limit; Effects of dilution, mass flow rate and inlet temperature'', ASME 2012 Gas Turbine India Conference, Mumbai, Maharashtra, India, Paper No. GTIndia2012-9742.

This paper was published based on the results of the first experimental campaign carried out using the variable-swirl combustor (version I). The aim of the campaign was twofold: First to study the effect of varying the operational parameters namely: swirl number, inlet air temperature and inlet air mass flow rate on lean blowout of methane (as a base fuel); and second to investigate the lean blowout limit of fuel mixtures comprising considerable amounts of diluents (CO_2 and N_2). Choice of fuel mixtures for this paper was made with relevance to utilization of biogas in gas turbine combustors.

My contribution: As the first author of the paper, I surveyed the literature and designed the experiments under supervision of Jens Klingmann. I performed the experiments and processed the results together with my master student Denny Clerini. I analyzed the results and wrote the paper together with Alessandro Schönborn.

II. **Parisa Sayad**, Alessandro Schönborn, Jens Klingmann, ''Experimental investigations of the lean blowout limit of different syngas mixtures in an atmospheric, premixed variable-swirl burner'', Energy & Fuels, 27 (5), pp 2783–2793, 2013.

This paper was focused on studying the lean blowout of various syngas mixtures in comparison with methane. The experiments were performed in the variable-swirl burner (version I) using different mixtures of CH_4, H_2, CO and N_2. The effect of swirl number on the lean blowout limit as well as on the behavior of the flame near the lean blowout limit was investigated. A perfectly stirred reactor model was used to reproduce the experimentally obtained lean blowout limits of the studied fuel mixtures.

My contribution: As the main author of the paper, I did the literature review on the topic, chose the composition of the fuel mixtures and designed the experiments under supervision of my supervisors, Jens Klingmann and Alessandro Schönborn. The experiments were performed with the help of Jens Klingmann and Alessandro Schönborn. The outcomes of the work were discussed and analyzed together with the co-authors. I wrote the paper and reviewed it based the comments of the co-authors.

III. **Parisa Sayad**, Alessandro Schönborn, Mao Li, Jens Klingmann, ''Visualisation of different flashback mechanisms for H_2/CH_4 mixtures in a variable-swirl burner'', Journal of Engineering for Gas Turbines and Power, 137(3), pp. 301507/1-9, 2015.

This paper was published based on the flashback experiments carried out in the variable-swirl burner (version II). The focus of this study was to visualize and study flame propagation in the optical premixing section at flashback limit under various flow conditions. This was achieved using high-speed OH^*-chemiluminescence imaging. The flow conditions in the combustor were altered by changing the swirl number from 0.0 to 0.66 and the total air mass flow rate from 75 to 200 SLPM. Varying the flow parameters was shown to have a significant effect on how the flame flashback was triggered for different mixtures of CH_4/H_2.

My contribution: As the main author of the paper, I did the literature review on the topic, chose the test conditions and designed the experiments under supervision of Jens Klingmann and Alessandro Schönborn. The experiments were performed with the help of Mao Li and Alessandro Schönborn. I processed the experimental results. The outcomes of the work were discussed and analyzed together with the co-authors. I wrote the paper and reviewed it based the comments of the co-authors.

IV. **Parisa Sayad**, Alessandro Schönborn, Jens Klingmann, ''Experimental investigation of the stability limits of premixed syngas-air flames at two moderate swirl numbers'', Combustion and Flame, 164, pp. 270-282, 2016.

This study was initiated based on the results obtained in the previous papers (Paper **II** and Paper **III**) regarding the effect of swirl number on the lean blowout and flashback limits of various fuel mixtures. According to previous experiments, the swirl number had a greater effect on the flashback equivalence ratio than on the lean blowout equivalence ratio of a given fuel mixture. Paper **V** was therefore aimed at investigating whether or not minor changes in the swirl number can extend the stability range of the combustor using various syngas mixtures. To this end, two moderate swirl numbers of 0.53 and 0.66 were studied. The flashback and lean blowout equivalence ratios of 17 different fuel mixtures comprising H_2, CO and CH_4 were measured. High-speed OH^*-chemiluminescence imaging and PIV technique were used to identify the differences between the two swirl numbers in terms of the flow field and flame behavior.

My contribution: As the main author of the paper, I decided on the fuel mixtures and the test conditions. I set up and designed the experiments. The experiments were performed with the help of my colleagues Mao Li and Yiheng Tong. I processed the experimental results. The outcomes of the work were discussed and analyzed together with the co-authors. I wrote the paper and revised it based the comments of the co-authors.

70

V. Alessandro Schönborn, **Parisa Sayad**, Jens Klingmann, ''Influence of precessing vortex core on flame flashback in swirling hydrogen flames'', International Journal of Hydrogen Energy, 39, pp. 20233-20241, 2014.

This study was initiated and planned based on the visual observations of flashback behavior from our previous study (Paper **III**). This study showed that the flame seemed to have a lower axial propagation speed when it displayed an eccentric motion around the central axis of the premixing section during flashback. The precessing vortex core can cause the eccentric motion of the flame. The presence of precessing vortex core can affect the flow and temperature field and hence the combustion behavior in the combustor. The focus of this paper was therefore to examine the influence of the flow eccentric motion on the direction and speed of a hydrogen/air flame during flashback. The experiments were performed in the variable-swirl burner (Version II) at three swirl numbers of 0.514, 0.594 and 0.66. The flow field in the combustor at these swirl numbers was characterized using PIV. High-speed OH^*-chemiluminescence was used to visualize the flame propagation in the premixing section during flashback. The radial position of the flame tip with respect to its axial position was estimated by thresholding the images. This enabled estimation of flame propagation speed in the premixing section. Considering the radial position of the flame in relation to its axial propagation speed it was concluded that as the eccentricity of the flame tip increased the flashback speed decreased. This suggested that flame eccentricity caused by precessing vortex core might have an inhibiting effect on flame flashback in swirl-stabilized combustors.

My contribution: As the second author of the paper I was involved in planning, setting up and performing the experiments. I actively took part in the discussions on the outcome of the experiments. The lead author wrote the paper; however, I helped with the structure of the paper and formulating the outcomes.

VI. Alessandro Schönborn, **Parisa Sayad**, Alexander A. Konnov, Jens Klingmann, ''Visualisation of propane autoignition in a turbulent flow reactor using OH^*-chemiluminescence imaging'', Combustion and Flame, 160(6), pp. 1033-1043, 2013.

This paper aimed at investigating the autoignition of propane/air mixtures in a turbulent flow reactor. Several autoignition events were visualized in the optical test section of the reactor using high-speed OH^*-chemiluminescence imaging. The OH^*-chemiluminescence images allowed for studying the spatial and temporal development of autoignition kernels. The ignition delays of propane/air mixtures were measured at various temperatures, equivalence ratios and pressures. In addition, the effect of CO_2 dilution on the ignition delays was studied. These parameters were chosen with relevance to micro-gas turbine conditions. The ignition delays were compared with the predictions of chemical kinetic models and experimental data previously reported in the literature. A chemical kinetic reactor

71

network model was developed to estimate the error, which was imposed on the measured ignition delays due to the finite mixing time of the reactant in the experimental set up.

My contribution: As the second author of the paper I was involved in performing the experiments. I actively took part in the discussions on the outcome of the experiments. I conducted the chemical kinetic modeling of the experimental results. I developed the chemical kinetic reactor network model that was used to estimate the mixing error on the experimental results. I was involved in writing the paper.

VII. Alessandro Schönborn, **Parisa Sayad**, Alexander A. Konnov, Jens Klingmann, ''OH*-chemiluminescence during autoignition of hydrogen with air in a pressurised turbulent flow reactor'', International Journal of Hydrogen Energy, 39(23), pp. 12166-12181, 2014.

This paper was focused on investigating the autoignition of H_2/air mixtures in a turbulent flow reactor. The objectives of the study were first, to visualize the autoignition process using OH*-chemiluminescence imaging and second, to measure the ignition delays of H_2/air at various pressures and temperatures and finally, to compare the experimental results with the predictions of chemical kinetic calculations. The analysis of the OH*-chemiluminescence images showed that the autoignition kernels formed in the central regions of the tube and subsequently expanded and merged through deflagration. Flashback occurred even though the turbulent flame speed was measured to be lower than the initial flow velocity in the reactor. Experiments showed that decreasing the pressure reduced the ignition delay of the reactants within the studied range. This trend was not predicted by the chemical kinetic calculations when using only homogeneous gas phase kinetics. For this reason, a kinetic model was altered to include surface reactions at the reactor walls. By considering the surface reactions, the calculations were reconciled with the experimental data. This indicated that wall reactions had a significant influence on ignition delays.

My contribution: As the second author of the paper, I was involved in performing the experiments. I actively took part in the discussions on the outcomes of the experiments. I conducted the chemical kinetic modeling of the experimental results. I altered a chemical kinetic model to include the surface reactions. The lead author wrote the paper; however, I helped with the structure of the paper and formulating the outcomes.

7. CONCLUDING REMARKS

This doctoral thesis has presented experimental investigations of lean blowout, flashback and autoignition in premixed combustion using alternative fuels with relevance to gas turbine combustors. The lean blowout and flashback experiments were conducted in an atmospheric variable-swirl combustor. The autoignition experiments were performed in a pressurized turbulent flow reactor. Several measurement techniques were used throughout this work such as LDA, PIV and high-speed OH^*-chemiluminescence imaging. The fuel mixtures consisted varying amounts of hydrogen, methane, carbon monoxide, nitrogen and carbon dioxide. Chemical kinetic modeling was used to understand the role of chemical processes in the studied combustion phenomena. The main conclusions of this work are:

- The swirl number had a significant role on the combustion behavior of various mixtures under stable operation as well as when approaching lean blowout and flashback limits.
- While the swirl number had a significant effect on flashback limits, it did not influence the lean blowout limits of various fuel mixtures as strongly. It was concluded that varying the swirl number may be a plausible way to extend the stability range of the combustor when using highly reactive fuels.
- The effect of swirl number on flashback and lean blowout limits became less pronounced when increasing the hydrogen content of the fuel mixtures
- Flashback can be triggered by different mechanisms in a given experimental setup depending on the flow field in the combustor.
- When the swirl number is in a moderate range and flame stabilization is achieved by a recirculation zone, the flashback mechanism may change as a result of small changes in the swirl number.
- Propagation speed of flashback varied significantly depending on the mechanism causing the flashback.
- The visual observations suggest that when flashback is caused by CIVB, it may be possible to change the flame propagation direction and send the flame back in to the combustor. This is not the case when flashback is initiated in the boundary layer.
- Catalytic wall reactions can cause autoignition at residence times well below the predictions of chemical kinetic models. Autoignition can cause flame propagation in the premixing section even when a lifted flame is present in the combustor.

73

The investigations performed throughout this thesis can be continued by following two potential pathways. The first pathway may be to focus on prediction of LBO/FB limits of various fuel mixtures using simplified chemical kinetic models. To do so, more data needs to be collected on the LBO and FB limits of various fuel mixtures. The data can then be used to find an empirical criterion that can correlate the experimental results with chemical kinetic models. The second pathway can be to focus on the LBO and FB mechanisms of high reactivity fuels over a narrower range of moderate swirl numbers. Simultaneous PIV / OH*-chemiluminescence imaging can provide more information on how the flame/flow interaction alters the stabilization mechanism and flashback mechanism at moderate swirl numbers.

References

[1] IEA, "Electricity Information 2015". IEA.

[2] IEA, "Resources to Reserves 2013". OECD Publishing.

[3] IEA, "CO2 Emissions from Fuel Combustion 2015". OECD Publishing.

[4] Mom, A.J.A., "1 - Introduction to gas turbines A2 - Jansohn, Peter", in Modern Gas Turbine Systems. 2013, Woodhead Publishing. p. 3-20.

[5] Gupta, K.K., Rehman, A., and Sarviya, R.M., "Bio-fuels for the gas turbine: A review". Renewable and Sustainable Energy Reviews, 2010. 14(9): p. 2946-2955.

[6] Moriarty, P. and Honnery, D., "A hydrogen standard for future energy accounting". International Journal of Hydrogen Energy, 2010. 35(22): p. 12374-12380.

[7] Flohr, P. and Stuttaford, P., "5 - Combustors in gas turbine systems A2 - Jansohn, Peter", in Modern Gas Turbine Systems. 2013, Woodhead Publishing. p. 151-191e.

[8] Huang, Y. and Yang, V., "Dynamics and stability of lean-premixed swirl-stabilized combustion". Progress in Energy and Combustion Science, 2009. 35(4): p. 293-364.

[9] Turns, S.R., "An introduction to combustion: concepts and applications". 1996: McGraw-Hill.

[10] Abdel-Gayed, R.G., Bradley, D., and Lung, F.K.K., "Combustion regimes and the straining of turbulent premixed flames". Combustion and Flame, 1989. 76(2): p. 213-218.

[11] Lefebvre, A.H., "Gas turbine combustion". Second ed. 1998: Taylor & Francis.

[12] Syred, N. and Beér, J.M., "Combustion in swirling flows: A review". Combustion and Flame, 1974. 23(2): p. 143-201.

[13] Smith, K.O., Kurzynske, F.R., and Angello, L.C. "Experimental evaluation of fuel injection configurations for a lean-premixed low NOx gas turbine combustor". 1987. ASME.

[14] Spalding, D.B., "Some fundumentals of combustion". 1955, New York: Academic Press

[15] Longwell, J.P., Frost, E.E., and Weiss, M.A., "Flame stability in bluff body recirculation zones". Industrial & Engineering Chemistry, 1953. 45(8): p. 1629-1633.

[16] Plee, S.L. and Mellor, A.M., "Characteristic time correlation for lean blowoff of bluff-body-stabilized flames". Combustion and Flame, 1979. 35(0): p. 61-80.

[17] Radhakrishnan, K., Heywood, J.B., and Tabaczynski, R.J., "Premixed turbulent flame blowoff velocity correlation based on coherent structures in turbulent flows". Combustion and Flame, 1981. 42(0): p. 19-33.

[18] Noble, D.R., Zhang, Q., Shareef, A., Tootle, J., Meyers, A., and Lieuwen, T. "Syngas mixture composition effects upon flashback and blowout". in Proceedings of ASME Turbo Expo. 2006. Barcelona, Spain: ASME.

[19] Lieuwen, T., McDonell, V., Petersen, E., and Santavicca, D., "Fuel flexibility influences on premixed combustor blowout, flashback, autoignition, and stability". Journal of Engineering for Gas Turbines and Power, 2008. 130(1): p. 011506-011506.

[20] Fritz, J., Kröner, M., and Sattelmayer, T. "Flashback in a swirl burner with cylindrical premixing zone". in Proceedings of ASME Turbo Expo. 2001. New Orleans, Louisiana, USA: ASME.

[21] Kröner, M., Sattelmayer, T., Fritz, J., Kiesewetter, F., and Hirsch, C., "Flame propagation in swirling flows—effect of local extinction on the combustion induced vortex breakdown". Combustion Science and Technology, 2007. 179(7): p. 1385-1416.

[22] Dam, B., Corona, G., Hayder, M., and Choudhuri, A., "Effects of syngas composition on combustion induced vortex breakdown (CIVB) flashback in a swirl stabilized combustor". Fuel, 2011. 90(11): p. 3274-3284.

[23] Dam, B., Love, N., and Choudhuri, A., "Flashback propensity of syngas fuels". Fuel, 2011. 90(2): p. 618-625.

[24] Sayad, P., Schönborn, A., Li, M., and Klingmann, J., "Visualization of different flashback mechanisms for H2/CH4 mixtures in a variable-swirl burner". Journal of Engineering for Gas Turbines and Power, 2014. 137(3): p. 031507-031507.

[25] Lewis, B. and Von Elbe, G., "Combustion, flames and explosion of gases". 1961, New York: Academic Press.

[26] Wohl, K. "Quenching, flash-back, blow-off-theory and experiment". in 4th Symposium (Int.) on Combustion. 1953. Pittsburgh, PA: The combustion Institute.

[27] Yamazaki, K. and Tsuji, H., "An experimental investigation on the stability of turbulent burner flames", in 8th Symposium (Int.) on Combustion1961, The combustion Institute: California. p. 543-553.

[28] Fine, B., "The flashback of laminar and turbulent burner flames at reduced pressure". Combustion and Flame, 1958. 2(3): p. 253-266.

[29] Umemura, A. and Tomita, K., "Rapid flame propagation in a vortex tube in perspective of vortex breakdown phenomena". Combustion and Flame, 2001. 125(1–2): p. 820-838.

[30] Fritz, J., Kröner, M., and Sattelmayer, T., "Flashback in a swirl burner with cylindrical premixing zone". Journal of Engineering for Gas Turbines and Power, 2004. 126(2): p. 276-283.

[31] Burmberger, S., Hirsch, C., and Sattelmayer, T. "Design rules for the velocity field of vortex breakdown swirl burners". in Proceedings of ASME Turbo Expo 2006. Barcelona, Spain: ASME.

[32] Kiesewetter, F., Konle, M., and Sattelmayer, T., "Analysis of combustion induced vortex breakdown driven flame flashback in a premix burner with cylindrical mixing zone". Journal of Engineering for Gas Turbines and Power, 2007. 129(4): p. 929-936.

76

[33] Konle, M. and Sattelmayer, T., "Interaction of heat release and vortex breakdown during flame flashback driven by combustion induced vortex breakdown". Experiments in Fluids, 2009. 47(4-5): p. 627-635.

[34] Darmofal, D.L., "The role of vorticity dynamics in vortex breakdown", in AIAA, Fluid Dynamics Conference, 24th1993: Orlando, FL. p. 15 p.

[35] Panton, R.L., "Incompressible flow". 1996, New York: John Wiley & Sons, Inc.

[36] Plee, S.L. and Mellor, A.M., "Review of flashback reported in prevaporizing/premixing combustors". Combustion and Flame, 1978. 32: p. 193-203.

[37] Beerer, D.J. and McDonell, V., "Autoignition of hydrogen and air inside a continuous flow reactor with application to lean premixed combustion". Journal of Engineering for Gas Turbines and Power, 2008. 130 (2008): p. 051507-051507-8.

[38] Glassman, I., "Combustion". Third ed. 1996, San Diego: Academic Press. 1-631.

[39] Griffiths, J.F. and Barnard, J.A., "Flame and Combustion". 1995: Taylor & Francis.

[40] Warnatz, J., Maas, U., and Dibble, R.W., "Combustion. Physical and chemical fundamentals, modeling and simulation, experiments, pollutant formation". 4th ed. 2006: Springer

[41] Kee, R.J., Coltrin, M.E., and Glarborg, P., "Chemically reacting flow, theory and practice". 2003, Hoboken, New Jersey: John Wiley & sons. 928.

[42] Beerer, D., McDonell, V., Samuelsen, S., and Angello, L., "An experimental ignition delay study of alkane mixtures in turbulent flows at elevated pressures and intermediate temperatures". Journal of Engineering for Gas Turbines and Power, 2010. 133(1): p. 011502-011502.

[43] "Spontaneous ignition delay characteristics of hydrocarbon fuel/air mixtures", National Aeronautics and Space Administration.

[44] Wu, H. and Ihme, M., "Effects of flow-field and mixture inhomogeneities on the ignition dynamics in continuous flow reactors". Combustion and Flame, 2014. 161(9): p. 2317-2326.

[45] Beerer, D.J. and McDonell, V.G., "An experimental and kinetic study of alkane autoignition at high pressures and intermediate temperatures". Proceedings of the Combustion Institute, 2011. 33(1): p. 301-307.

[46] "Blending hydrogen into natural gas pipeline networks: A review of key issues", technical report, National Renewable Energy Laboratory.

[47] Chiesa, P., Lozza, G., and Mazzocchi, L., "Using hydrogen as gas turbine fuel". Journal of Engineering for Gas Turbines and Power, 2005. 127(1): p. 73-80.

[48] Fatehi, H. and Bai, X.S., "A comprehensive mathematical model for biomass combustion". Combustion Science and Technology, 2014. 186(4-5): p. 574-593.

[49] Huth, M. and Heilos, A., "14 - Fuel flexibility in gas turbine systems: impact on burner design and performance A2 - Jansohn, Peter", in Modern Gas Turbine Systems. 2013, Woodhead Publishing. p. 635-684.

[50] Haugen, N.E.L., Brunhuber, C., and Bysveen, M., "Hydrogen fuel supply system and re-heat gas turbine combustion". Energy Procedia, 2012. 23(0): p. 151-160.

[51] Lieuwen, T., McDonell, V., Santavicca, D., and Sattelmayer, T., "Burner development and operability issues associated with steady flowing syngas fired combustors". Combustion Science and Technology, 2008. 180(6): p. 1169-1192.

[52] Bird, R.B., Stewart, W.E., and Lightfoot, E.N., "Transport phenomena". second ed. 2001, New York: John Wiley & Sons, Inc.

[53] Kang, D.W., Kim, T.S., Hur, K.B., and Park, J.K., "The effect of firing biogas on the performance and operating characteristics of simple and recuperative cycle gas turbine combined heat and power systems". Applied Energy, 2012. 93(0): p. 215-228.

[54] Qin, W., Egolfopoulos, F.N., and Tsotsis, T.T., "Fundamental and environmental aspects of landfill gas utilization for power generation". Chemical Engineering Journal, 2001. 82(1–3): p. 157-172.

[55] Takamori, S. and Umemura, A., "Behaviors of a flame ignited by a hot spot in a combustible vortex (vortex-bursting initiation revisited)". Proceedings of the Combustion Institute, 2002. 29(2): p. 1729-1736.

[56] Kröner, M., Fritz, J., and Sattelmayer, T., "Flashback limits for combustion induced vortex breakdown in a swirl burner". Journal of Engineering for Gas Turbines and Power, 2003. 125(3): p. 693-700.

[57] Design, R., "Chemkin", in 101122010, Reaction Design: San Diego.

[58] Sayad, P., Schönborn, A., and Klingmann, J., "Experimental Investigations of the Lean Blowout Limit of Different Syngas Mixtures in an Atmospheric, Premixed, Variable-Swirl Burner". Energy & Fuels, 2013.

[59] Schönborn, A., Sayad, P., Konnov, A.A., and Klingmann, J., "Visualisation of propane autoignition in a turbulent flow reactor using OH* chemiluminescence imaging". Combustion and Flame, 2013. 160(6): p. 1033-1043.

[60] Zhang, Z., "LDA application methods". 1 ed. Experimental Fluid Mechanics, ed. W.R. Merzkirch, Donald; Tropea, Cameron. 2010, Heidelberg: Springer-Verlag Berlin Heidelberg.

[61] Durst, F., Melling, A., and Whitelaw, J.H., "Principles and practice of laser-Doppler anemometry". 1976: Academic Press.

[62] Eckbreth, A.C., "Laser diagnostics for combustion temperature and species". 1996: Taylor & Francis.

[63] "Dantec Dynamics, Laser Doppler Anemometry : Introduction to principles and applications". Available from: http://www.dantecdynamics.com/educational-slideshows.

[64] Melling, A., "Tracer particles and seeding for particle image velocimetry". Measurement Science and Technology, 1997. 8(12).

[65] LaVision, "Flow Master", in Product Manual for DaVis 8.1, LaVision: Gottingen, Germany.

[66] Raffel, M., Willert, C.E., Wereley, S., and Kompenhans, J., "Particle image velocimetry: A practical guide". 2 ed. 2007, Heidelberg: Springer.

[67] Dabiri, D., "Digital particle image thermometry/velocimetry: A review". Experiments in Fluids, 2009. 46(2).

[68] Chen, j. and Katz, J., "Elimination of peak-locking error in PIV analysis using the correlation mapping method". Measurement Science and Technology, 2005. 16(8).

[69] Sayad, P., Schönborn, A., and Klingmann, J., "Experimental investigation of the stability limits of premixed syngas-air flames at two moderate swirl numbers". Combustion and Flame, 2016. 164: p. 270-282.

78

[70] Nori, V. and Seitzman, J., "Evaluation of chemiluminescence as a combustion diagnostic under varying operating conditions ", in 46th AIAA Aerospace Sciences Meeting and Exhibit2008, American Institute of Aeronautics and Astronautics Reno, Nevada. p. 14.

[71] Schönborn, A., Sayad, P., Konnov, A.A., and Klingmann, J., "OH*-chemiluminescence during autoignition of hydrogen with air in a pressurised turbulent flow reactor". International Journal of Hydrogen Energy, 2014. 39(23): p. 12166-12181.

[72] Deutschmann, O., Schmidt, R., Behrendt, F., and Warnat, J., "Numerical modeling of catalytic ignition". Symposium (International) on Combustion, 1996. 26(1): p. 1747-1754.